REPORT DOCUMENTATION PAGE

Form Approved
OMB NO. 0704-0188

Public reporting burden for this collection of information is estimated to average 1 hour per response, including the time for reviewing instructions, searching, gathering and maintaining the data needed, and completing and reviewing the collection of information. Send comments regarding this burden estimate or any other aspect of this collection of information, including suggestions for reducing this burden to Washington Headquarters Services, Directorate for Information Operations and Reports, 1215 Jefferson Davis Highway, Suite 1204, Arlington, VA 22202-4302, and to the office of Management and Budget, Paperwork Reduction Project (0704-0188), Washington, DC 20503.
PLEASE DO NOT RETURN YOUR FORM TO THE ABOVE ADDRESS.

1.REPORT DATE (MM-DD-YYYY)	2.REPORT TYPE	3. DATES COVERED
10/25/05	ANNUAL	10/01/2004 - 09/30/2005

4. TITLE AND SUBTITLE
Predictive Computations of Properties of Wide-Gap and Nano-Semiconductors

5a. CONTRACT NUMBER

5b. GRANT NUMBER
N00014-05-1-0009

5c. PROGRAM ELEMENT NUMBER

6. AUTHOR (S)
DIOLA BAGAYOKO, PH.D., PROJECT DIRECTOR
G. L. ZHAO, PH.D., CO-PRINCIPAL INVESTIGATOR

5d. PROJECT NUMBER

5e. TASK NUMBER

5f. WORK UNIT NUMBER

7. PERFORMING ORGANIZATION NAME (S) AND ADDRESS (ES)
Southern University and A & M College, Office of Research, 500 Harding Boulevard, Baton Rouge, LA 70813

8. PERFORMING ORGANIZATION REPORT NUMBER

9. SPONSORING/MENTORING AGENCY NAME (S) AND ADDRESS (ES)
THE DEPARTMENT OF THE NAVY, OFFICE OF NAVAL RESEARCH (ONR), ATTENTION: DR. COLIN E. WOOD, TECHNICAL REPRESENTATIVE BALLSTON CENTRE TOWER ONE, 800 NORTH QUINCY STREET, ARLINGTON, VA 22217-5660

10.SPONSOR/MONITOR'S ACRONYM (S)
ONR

11.SPONSOR/MONITOR'S REPORT NUMBER (S)

12. DISTRIBUTION/AVAILABILITY STATEMENT
UNLIMITED

13. SUPPLEMENTARY NOTES

14. ABSTRACT
We report the progress made in the implementation of the aforementioned project. To date, we have strictly adhered to the provisions in the proposal relative to the research personnel, materials under study (i.e., GaN, InN, ZnO, Carbon Nanotubes), and the overall research tasks (i.e., computations and theoretical analysis). We have consequently generated new knowledge that is reported in several articles. Six (6) of these articles have already been published, with three (3) in refereed journals and three (3) in refereed conference proceedings. These article are appended to this report. We have made seven (7) technical presentations on our findings at two (2) national and one (1) international conferences. The utter significance of our findings resides in the fact that they have confirmed our resolution of a long-standing problem in materials science stemming from a woeful underestimation, by theory, of the measured energy gaps (atoms, molecules, and clusters) and band gaps (semiconductors and insulators). Specifically, density functional theory (DFT) and its local density approximation (LDA) had been blamed, before our work, for the resulting gross disagreements between theory and experiment. Unlike previous works, we have obtained the experimentally measured band gaps of wurtzite InN, ZnO, and of several single walled carbon nanotubes. This feat was accomplished by our utilization of the Bagayoko, Zhao, and Williams (BZW) method. Further, we have predicted the band gap of cubic InN for which no experimental results are available. It is befitting that this ONR funded project exonerated DFT and LDA that were obtained by a project funded by ONR and for which Dr. Walter Kohn received the 1998 Nobel Prize in Chemistry. *With the BZW method, DFT and LDA calculations can now predict the energy or band gaps of materials, from atoms and molecules to semiconductors and insulators.* The importance of this point cannot be overemphasized in light of the currency of nanoscience and technology: indeed, at the nanoscale, accurately calculated energy or band gaps are indispensable in informing and in guiding device design and fabrication. Incidentally, the above feat of the BZW method should apply to nuclei in the shell model!

15. SUBJECT TERMS: DENSITY FUNCTIONAL THEORY; LOCAL DENSITY APPROXIMATION; BAGAYOKO, ZHAO, AND WILLIAMS (BZW) METHOD; PREDICTION OF ELECTRONIC PROPERTIES, INCLUDING ENERGY OR BAND GAPS; RAYLEIGHT-RITZ VARIATIONAL METHOD; LINEAR COMBINATION OF ATOMIC ORBITAL (LCAO).

16. SECURITY CLASSIFICATION OF: UNCLASSIFIED			17. LIMITATION OF ABSTRACT	18.NUMBER OF PAGES	19a. NAME OF RESPONSIBLE PERSON
a. REPORT	b. ABSTRACT	c. THIS PAGE	UU	40	DIOLA BAGAYOKO, PH.D.
					19b. TELEPHONE NUMBER (Include area code) (225) 771-2730

ANNUAL REPORT

GRANT#: N00014-05-1-0009

PRINCIPAL INVESTIGATORS: Diola Bagayoko, Ph.D., Southern University System Distinguished Professor of Physics, Project Director, and G. L. Zhao, Ph.D., Associate Professor of Physics, SUBR, Co-Principal Investigator

Program Officer, Office of Naval Research (ONR): Colin E. Wood, Ph.D., Ballston Centre tower One, 800 North Quincy Street, Arlington, VA 22217-5660

INSTITUTION: Southern University and A & M College in Baton Rouge (SUBR)

GRANT TITLE: Predictive Computations of Properties of Wide-Gap and Nano-Semiconductors

AWARD PERIOD: October 1, 2004 to September 30, 2005

OBJECTIVE: As per the initial proposal, the aim of this project is (a) to produce new scientific knowledge on wide-gap and nano-semiconductors, with specific materials including GaN, InN, AlN, and carbon nanotubes, (b) to develop analytical and computational techniques and computer codes for wider applications in descriptive and predictive investigations of the above materials and others, and (c) to provide research training for undergraduate and graduate students, including minority students at SUBR.

APPROACH: Our *technical approach or method*, as per the proposal, consists of the following. Like most previous calculations of electronic and related properties of semiconductors, we employ a density functional theory (DFT) potential. This potential is often selected, by design, from the local density approximation (LDA) to the general DFT. We also utilize, like previous works, the linear combination of atomic orbital (LCAO) formalism in a Rayleigh-Ritz variational procedure to perform self-consistent calculations. Our calculations, to date, are for zero temperature and are non-relativistic.

The key distinction between our method and those of all previous calculations by other groups resides in our adherence to the Bagayoko, Zhao, and Williams (BZW) method in the implementation of the LCAO formalism. References clearly identified in the attached articles fully describe this method. *Essentially, this method resolved the long-standing underestimation, by theory, of measured energy or band gaps of finite (atoms, clusters, molecules) and infinite (semiconductors insulators) systems.* As explained in the attached articles and references therein, BZW first identified a basis set and variational effect that is responsible for an unphysical lowering of the low-lying, unoccupied energy levels or bands of materials. This unphysical lowering is shown to be a mathematical artifact stemming from the Rayleigh theorem. BZW subsequently introduced a rigorous method of performing variational calculations in such a way that the above unphysical lowering of unoccupied levels or bands is totally avoided. *Let us underscore that the underestimation of energy and band gaps is a trivial consequence of the above unphysical lowering of unoccupied levels of bands.*

20051028 017

The BZW method generally entails the performance of three (3) or more self-consistent calculations. The first calculation employs the minimal basis set for the system and progressively augment it in subsequent calculations. The **occupied** energy levels or bands of a calculation the next, consecutive calculation whose basis set is larger. As explained in detail in the articles, successive calculations have different basis sets: the basis set for the latter is obtained by augmenting that of the former with the next excited state orbital an atomic or ionic species that is present in the system under study (i.e., In and N for InN). This process continues until the occupied energies are found to be identical for two consecutive calculation N and (N+1). Then, the results of calculation N are the physical ones for the system under study (and not those of calculation N+1). This criterion for stopping the process rests trivially on the facts that (a) density functional theory is a ground state theory and (b) only the wave functions of the occupied states are including in the construction and reconstruction of the charge density (and hence the potential and the Hamiltonian) in the self-consistency process.

Once the correct energy levels or bands are obtained, then we proceed to calculate a host of properties that include the energy or band gaps, optical transition energies, the total energy, the total and partial densities of states, the effective masses of charge carriers (for application in transport studies), and the optical properties (i.e., the complex dielectric functions). Of course, the total energy curves are utilized to compute the bulk modulus.

In addition to the above *technical approach*, we should note that our programmatic implementation also adhered to the proposal. In particular, we have hired Dr. Hua Jin as the Postdoctoral Associate. She has been performing excellently, not only in carrying out research tasks, but also in assisting the investigators in their training of students on the complex software package utilized in this work. A graduate and undergraduate students, mostly African American, have also been employed. SUBR is a Historically Black College and University (HBCU). The effort levels of the investigators (D. Bagayoko and G. L. Zhao) are as per the proposal.

ACCOMPLISHMENTS: As summarized in the abstract of this report, we have published six (6) articles, made seven (7) technical presentations, two of which were at an international conference. A seventh article is pending. To reduce redundancy, we refer the reader to the following full listing of the articles, with referencing information. We also list the presentations below. The subtitles below, for accomplishments, are keyed to the objectives enunciated above.

Publications

"Structural, Elastic, and Electronic Properties of Deformed Carbon Nanotubes under Uniaxial Strain." A. Pullen, G. L. Zhao, D. Bagayoko, and L. Yang. Physical Review B 71, 205410.

"Ab-initio Simulations of the Growth and Structural Properties of Short Carbon Nanobells." G. L. Zhao, D. Bagayoko, and E. G. Wang. Accepted for publication in the Proceedings of the 2005 China Conference on Nanoscience and Technology, Beijing, China, July 2005.

"A Universal Relation Between the Densities of States Near van Hove Singularities and the Effective Electron Masses in 1-Dimensional Semiconductors." G. L. Zhao and D. Bagayoko. Accepted for publication in the Proceedings of the 2005 China Conference on Nano-Science and Technology , Beijing, China, July 2005.

"LDA and LCAO-BZW Description of Electronic Properties of Wurtzite Zinc Oxide (w-ZnO)." Diola Bagayoko, Lashounda Franklin, and G. L. Zhao, accepted for publications in Proceedings of the 2005 National Conference of the National Society of Black Physicists (www.nsbp.org), Orlando, Florida.

"Predictions of Electronic, Structural, and Elastic Properties of Cubic InN." Diola Bagayoko, Lashounda Franklin, and G. L. Zhao, Journal of Applied Physics 96, 4297-4301, 2004.

"Density Functional Band Gap of Wurtzite InN." Diola Bagayoko and Lashounda Franklin, Journal of Applied Physics, 97, 123708, 2005.

"Re-examination of the Ab-initio Calculation of the Electronic Structures of ZnSe, Ge, and GaAs." G. L. Zhao, L. Franklin, and D. Bagayoko. Submitted to Physical Review B, 2005.

Presentations

June 9-11, 2005, Beijing, China. China International Conference on Nanoscience and Technology. *"Ab-initio Simulations of the Growth and Structural Properties of Short Carbon Nanobells."* G. L. Zhao, D. Bagayoko, and E. G. Wang.

June 9-11, 2005, Beijing, China. China International Conference on Nanoscience and Technology. *"A Universal Relation Between the Densities of States Near van Hove Singularities and the Effective Electron Masses in 1-Dimensional Semiconductors."* G. L. Zhao and D. Bagayoko.

March 25, 2005. Los Angeles, CA. March Meeting of the American Physical Society (APS). *"Structural, Elastic, and Electronic Properties of Deformed Carbon Nanotubes under Uniaxial Strain." A. Pullen SUBR & (Caltech),* G. L. Zhao, D. Bagayoko, and L. Yang (NASA), Bull. APS, Vol. 50, No. 1, Page 1420 (2005).

March 23, 2005. Los Angeles, CA. March Meeting of the American Physical Society (APS). *"Re-examination of Ab-initio Calculation of the Electronic Structure of Zn Se, Ge, and GaAs."* G. L. Zhao, L. Franklin, and D. Bagayoko, Bull. APS, Vol. 50, No. 1, Page 1073 (2005).

March 22, 2005. Los Angeles, CA. March Meeting of the American Physical Society (APS). *"True LDA Band Gaps of Wurtzite and Cubic Indium Nitride (w-InN and c-InN)."* D. Bagayoko, G. L. Zhao, and L. Franklin. Bull. APS, Vol. 50, No. 1, Page 617 (2005). Audience: Approximately 70 physical science researchers and graduate students.

February 18, 2005. Orlando, Florida, Disneyland. 2005 National Conference of the National Society of Black Physicists (NSBP) and of the National Society of Hispanic Physicists (NSHP). *"Local Density Functional Description of Electronic Properties of Wurtzite Zinc Oxide (ZnO)."* D. Bagayoko, G. L. Zhao, and L. Franklin. Audience: 17 faculty members, graduate students, and federal lab researchers.

February 17, 2005. Orlando, Florida, Disneyland. 2005 National Conference of the National Society of Black Physicists (NSBP) and of the National Society of Hispanic Physicists (NSHP). *"A Competitive Edge for Recruitment: The Versatility and Wonders of Physics."* D. Bagayoko. Audience: 20 faculty members, graduate students, and federal lab researchers.

Code Development

Another major component of our accomplishments in this reporting period stems from the development and refinement of the computer program package for wider utilization. We have developed a precise and concise user-manual that we are currently field-testing for effectiveness.

Research Training of Students

We have trained four (4) minority undergraduate students in the performance of the sophisticated calculations this project entails. These students are physics majors at SUBR. One of the students is the first author on the Physical Review article on electronic, elastic, and related properties of single walled carbon nanotubes.

CONCLUSIONS: We have implemented in a successful manner, as gauged by the publications and technical presentations, this project focused on "predictive calculations of properties of wide-gap and nano-semiconductors. Materials studied to date include GaN, ZnO, wurtzite InN, cubic InN, and several carbon nanotubes. Our results, in contrast to previous DFT or LDA calculations by other groups, are in excellent agreement with experiment. The significance of these results is underscored below and in the abstract.

SIGNIFICANCE: Our articles on electronic, structural, optical, and other properties of semiconductors and carbon nanotubes (Please see the attached list of publications) have profound implications, even for the study of nuclei. These papers resolved a problem dating back to the beginning of quantum. Indeed, we solved the woeful, theoretical underestimation of the band gaps of semiconductors and insulators as compared to measured values. **The resolution of this problem has some serious implications for the design and fabrication of semiconductor-based and nano-devices.** A collateral benefit stems from the fact that the method of solution also applies to the prediction of nuclear energy levels in the shell model, opening the way to theoretical explorations of possibilities of a population inversion and the actual construction of a *"gamma ray amplification by stimulated emission of radiation (graser)" device. We believe that no comments are needed on commercial and other applications of a graser.*

PATENT INFORMATION: Not Applicable

AWARD INFORMATION: Not Applicable

ATTACHMENTS: FULL TEXT OF PUBLICATIONS LISTED ABOVE

LIST OF PUBLICATIONS

Annual Report
Grant No. N00014-05-1-0009
D. Bagayoko, Ph.D., and G. L. Zhao, Ph.D.
Department of Physics
Southern University and A&M College

Full copies of the following articles are provided below, in the order in which they are listed

"Structural, Elastic, and Electronic Properties of Deformed Carbon Nanotubes under Uniaxial Strain." A. Pullen, G. L. Zhao, D. Bagayoko, and L. Yang. Physical Review B 71, 205410.

"Ab-initio Simulations of the Growth and Structural Properties of Short Carbon Nanobells." G. L. Zhao, D. Bagayoko, and E. G. Wang. Accepted for publication in the Proceedings of the 2005 China Conference on Nanoscience and Technology, Beijing, China, July 2005.

"A Universal Relation Between the Densities of States Near van Hove Singularities and the Effective Electron Masses in 1-Dimensional Semiconductors." G. L. Zhao and D. Bagayoko. Accepted for publication in the Proceedings of the 2005 China Conference on Nano-Science and Technology , Beijing, China, July 2005.

"LDA and LCAO-BZW Description of Electronic Properties of Wurtzite Zinc Oxide (w-ZnO)." Diola Bagayoko, Lashounda Franklin, and G. L. Zhao, accepted for publications in Proceedings of the 2005 National Conference of the National Society of Black Physicists (www.nsbp.org), Orlando, Florida.

"Predictions of Electronic, Structural, and Elastic Properties of Cubic InN." Diola Bagayoko, Lashounda Franklin, and G. L. Zhao, Journal of Applied Physics 96, 4297-4301, 2004.

"Density Functional Band Gap of Wurtzite InN." Diola Bagayoko and Lashounda Franklin, Journal of Applied Physics, 97, 123708, 2005.

"Re-examination of the Ab-initio Calculation of the Electronic Structures of ZnSe, Ge, and GaAs." G. L. Zhao, L. Franklin, and D. Bagayoko. Submitted to Physical Review B, 2005.

Structural, elastic, and electronic properties of deformed carbon nanotubes under uniaxial strain

A. Pullen,[1] G. L. Zhao,[1,*] D. Bagayoko,[1] and L. Yang[2]
[1]*Department of Physics, Southern University and A & M College, Baton Rouge, Louisiana 70813, USA*
[2]*Eloret, NASA Ames Research Center, MS230-3, Moffett Field, California 94035, USA*
(Received 7 May 2004; revised manuscript received 20 January 2005; published 25 May 2005)

We report structural, elastic, and electronic properties of selected, deformed, single-wall carbon nanotubes under uniaxial strain. We utilized a generalized gradient approximation potential of density functional theory and the linear combination of atomic orbital formalism. We discuss bond-lengths, tubule radii, and the band gaps as functions of tension and compression strain for carbon nanotubes (10, 0), (8, 4), and (10, 10) which have chiral angles of 0, 19.1, and 30 deg relative to the zigzag direction. We also calculated the Young's modulus and the in-plane stiffness for each of these three nanotubes as representatives of zigzag, chiral, and armchair nanotubes, respectively. We found that these carbon nanotubes have unique structural properties consisting of a strong tendency to retain their tubule radii under large tension and compression strains.

DOI: 10.1103/PhysRevB.71.205410 PACS number(s): 73.22.−f, 61.46.+w

Single-wall carbon nanotubes (SWCNTs) can be viewed as rolled-up graphene sheets that have a diameter at the order of 1 nm. They have properties such as high current density, high elasticity, and stiffness unparalleled by other materials. Their potential applications range from that in building skyscrapers and elevator cables to the ones in very tiny electrical circuits and machines.[1] These materials, however, are too small for many conventional measurements. This situation underscores the possible importance of theoretical studies, including the one reported here that focuses on structural, elastic, and electronic properties of selected single-wall carbon nanotubes under uniaxial strain.

In the last several years, tight-binding calculations have been extensively used to study the structural and electronic structure of carbon nanotubes.[2–6] Tight-binding approximations based on the symmetry of the honeycomb lattice of graphite predicted that SWCNTs could be semiconducting or metallic depending on their chirality (n,m). The tight-binding model has been able to provide good estimates of the basic electronic structure of SWCNTs. However, curvature-related effects and the hybridization of different electronic states of graphite could lead to structural and electronic properties that are substantially different from the result of tight-binding calculations. Zigzag $(n,0)$ (where n is a multiple of 3) SWCNTs which were predicted to be metallic from tight-binding calculations were found to have small energy gaps.[7] Several theoretical groups have studied the elastic properties of carbon nanotubes. Their approaches include simulations with realistic many-body potentials,[8] the empirical force-constant method,[9] tight-binding formalisms,[6,10] pseudopotential calculations with local density approximation potentials,[11] and Born's perturbation technique within a lattice dynamics model.[12]

The aim of this work is therefore to study the aforementioned properties of SWCNTs, utilizing *ab initio* quantum computations. We specifically report on structural, elastic, and electronic properties of SWCNTs under uniaxial strain. Recent tight-binding calculations have led to values of bond lengths and radii, band gaps, and Fermi levels as functions of strain.[6] The dependence of tight-binding results upon the selected parameters partly suggests the present work that employs an *ab initio* approach.

Three main features characterize our first-principles computational method. The first of these features is the choice of the potential. We utilized the generalized gradient approximation (GGA) potential of Perdew and Wang.[13] This density functional[14–16] potential goes beyond the local density approximation (LDA). We also performed LDA calculations for carbon nanotube (10, 0). The second feature of our method stems from employing the linear combination of atomic orbital (LCAO). The third and distinctive feature of our work resides in our use of optimal basis sets as per the Bagayoko, Zhao, and Williams (BZW) procedure.[17–20] As explained elsewhere, this procedure avoids a basis set and variational effect inherently associated with variational calculations that employ a basis set and leads to the calculated band gaps in very good agreement with experiments.[17–20] With the above method, we solved the Kohn-Sham[14,15] equation self-consistently. Self-consistency was followed by the calculations of the total energies. Details of these steps, including the Kohn-Sham equation and the expression for the total energy, are fully described in the literature.[14–20]

In the LCAO method, we expanded the electronic eigenfunction Ψ_{ki} of the many-atom system as a linear combination of atomic wave functions.[17] These input functions result from *ab initio* calculations for atomic species that are present in the system. For the calculations, the C($1s$) state was used as the core state. For the (10, 0) and the (8, 4) tubes, the C($2s2p$) states were used as filled and partially filled valence states. The C($3s3p$) orbitals were the unfilled electron states that were used to augment the basis set for the calculations. For the (10, 10) tube, the C($2s2p$) states were used as filled and partially filled valence states and the C($3s$) as the unfilled state. The empty C($3p$) state was dropped, in the case of (10, 10), due to convergence difficulties.

Uniaxial strain was simulated by linearly scaling the atom positions along the tube axis in the carbon nanotube. To find how the tube radius changes with uniaxial strain, after the tube axis was scaled, the radius was identified from the total energy minimization procedure. Namely, for a given nano-

 ©2005 The American Physical Society

TABLE I. Unstrained bond lengths (a_0, b_0, and c_0) in carbon nanotubes (10,0), (8,4), and (10,10). L_0 is the length of the unit cell; r_0 is the tube radius; and N is the number of atoms per unit cell.

	(10,0)	(8,4)	(10,10)
a_0 (Å)	1.416	1.414	1.420
b_0 (Å)	1.416	1.419	1.420
c_0 (Å)	1.420	1.420	1.418
r_0 (Å)	3.915	4.143	6.781
L_0 (Å)	4.26	11.27	2.46
N	40	112	40

tube and a given compression or tensile strain, the total energy was obtained as a function of the tube radius. The equilibrium radius, i.e., the stable one, was the one corresponding to the minimum of the total energy. This process was repeated for each strain to obtain the radius of a tubule as a function of compression or tensile strain. Similarly, the calculated bond lengths, band gap, and Fermi energies, for a given nanotube and a given strain, are the one corresponding to the minimum of the total energies.

The Young's modulus for each SWCNT was calculated by fitting the total energy/unit cell for each strain ε_{zz} to the equation

$$E=\left[\frac{1}{2}\pi r^2 z Y\right]\varepsilon_{zz}^2, \tag{1}$$

where Y is the Young's modulus, z is the unit cell length, and r is the outer radius of the nanotube. Equation (1) was derived using the assumption that the nanotube was a perfect cylinder.[21] The standard radii tabulated for the nanotubes are for circumferences through the centers of the outer atoms. The outer radius includes such a standard radius plus the radius of the carbon atom (0.71 Å). We also calculated the in-plane stiffness C, which is an alternative measure of the mechanical characteristic of nanotubes that is defined as[22]

$$C=\frac{1}{S}\frac{\partial^2 E}{\partial \varepsilon_{zz}^2}, \tag{2}$$

where S is the surface area of the nanotube.

Table I displays the unstrained bond lengths and other characteristics of the tubules under study. In a graphene sheet, the lengths of the a, b, and c bonds are equal. In unstrained nanotubes, which are rolled graphene sheets, the three bonds are generally different. For the SWCNT (10, 0), the c bond along the axis is greater than the a and b bonds along the circumference ($a=b<c$). For the SWCNT (10, 10), the c bond along the circumference is shorter than the a and b bonds along the axis ($a=b>c$). In the case of the SWCNT (8, 4), the a bond closest to the circumference is less than the c bond closest to the axis, i.e., $a<b<c$. The bond lengths and radii as functions of the compression or tensile strain are displayed in Fig. 1 for the (10, 0) and Fig. 2 for the (8, 4). The calculated results for (10, 10) are very similar to those of (10, 0) and (8, 4) and are not presented in a separate figure, due to the page limitation of this brief

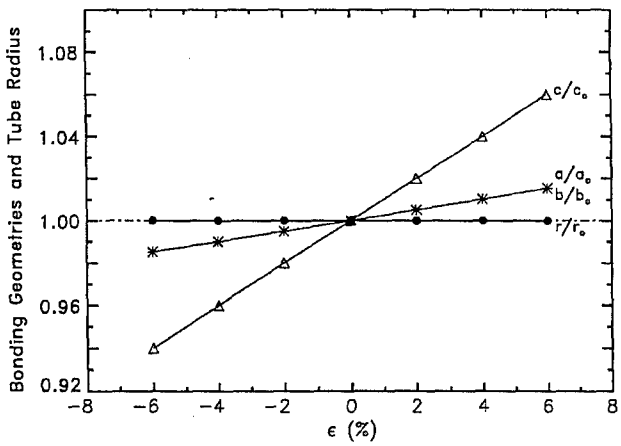

FIG. 1. Bond lengths and tube radius as functions of compression and tension strain ε for (10,0) nanotube. Each length is scaled to its unstrained length.

report. As per Figs. 1 and 2, the calculated and normalized lengths (i.e., a/a_0, b/b_0, or c/c_0) of bonds with a component along the axis decrease or increase linearly with compression or tensile strain, respectively. These variations are quantified with the slopes m provided in Table II.

A special feature of the calculated properties of the carbon nanotubes was that the radii of the nanotubes do not change under a substantially large uniaxial strain, from −6% to +6%. The Poisson's ratio, which is the ratio of the transverse contracting strain to the longitudinal elongational strain, is nearly zero for these carbon nanotubes. This behavior is drastically different from that of macroscopic materials and it disagrees with results of tight-bonding calculations and other mechanics simulations.[6,23] One possible explanation is that the bonds along the circumference, partly strengthened by curvature effects, are not significantly affected by uniaxial strains orthogonal to them (i.e., along the axis). We also repeated the studies using *ab initio* LDA calculations for SWCNT (10, 0). The total energy minimization of the LDA calculations for (10, 0) found the bond length at 1.402 Å for

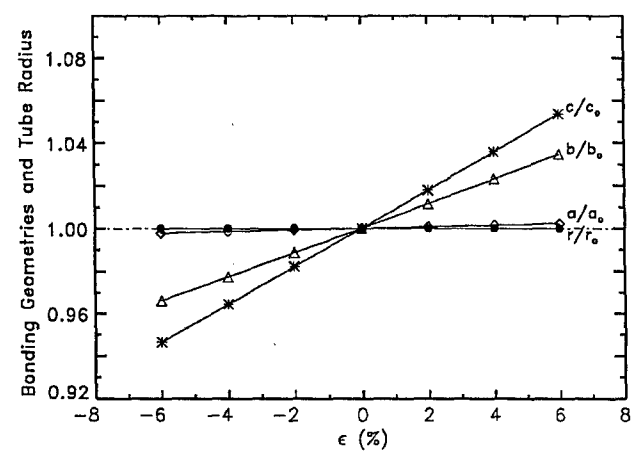

FIG. 2. Bond lengths and tube radius as functions of tension strain and compression strain ε for (8,4) nanotube. Each length is scaled to its unstrained length.

TABLE II. Coefficients m of linear variation of normalized bond lengths with compression (negative) and tensile (positive) strain (i.e., ε expressed as −0.04 and +0.06 for 4% and 6% compression and tensile strain, respectively). $\Delta 1/1_0 = m\varepsilon$, where 1 is the a, b, or c bond length. The Young's modulus Y is in TPa. The in-plane stiffness C is in J/m^2.

Nanotubes	m for bond a	m for bond b	m for bond c	Y (TPa)	C (J/m^2)
(10,0)	0.252	0.252	1.000	1.47	340
(8,4)	0.036	0.572	0.893	1.10	267
(10,10)	0.746	0.746	0[a]	0.726	272

[a]Bond c, for (10,10), is along the circumference of the tube.

a_0 and b_0 and 1.406 Å for c_0, that is about 1% smaller than the results of the *ab initio* GGA calculations. The *ab initio* LDA calculations for SWCNT (10, 0) also found that the radii of the nanotube did not change under a substantially large uniaxial strain. Among the previous *ab initio* calculations of the elastic properties of carbon nanotubes, Sanchez-Portal *et al.* utilized a minimal basis set of one s and three p orbitals per carbon atom and performed LDA calculations.[24] In their calculations, they used pseudoatomic orbitals.[24] Van Lier *et al.* utilized *ab initio* Hartree-Fock 6-31G method and closed nanotube models in their simulations.[25] Sanchez-Portal *et al.*[24] and Van Lier *et al.*[25] reported relatively small values (from 0.14 to 0.19) of the Poisson ratio for their calculated carbon nanotubes, which also indicated the diameter rigidity of the carbon nanotubes. These previous *ab initio* calculations utilized different computational methods, such as a minimal basis set and the Hartree-Fock method, and their results are slightly different from ours. As demonstrated in one of our previous publications,[30] the use of a minimal basis set may not be sufficient to obtain a highly accurate solution of the calculated electronic structure of the carbon nanotubes, which could explain in part the difference between our results and those of Sanchez-Portal *et al.* The fundamental differences between the Hartree-Fock method and density functional methods, i.e., the inclusion of the electronic correlation effects in the latter, partly explain the difference between our results and those of Van Lier *et al.* In our *ab initio* calculations, we utilized extended atomic basis sets and performed both GGA and LDA computations.

The calculated Young's moduli Y (in TPa) for the tubes are shown in Table II. We recall that the radius included in the formula for the Young's modulus is from the center of the tube to the outer circumference. This value of the radius led to Young's moduli close to the experimentally found value of approximately 1 TPa.[9] The (10, 0) and (10, 10) tubes have the highest and lowest Young's moduli, respectively. This trend is expected due to the bond geometry of the tubes according to chirality. All three bonds in the (10, 0) tube have a significant component parallel to the axis along which strain is applied. In the case of (10, 0), the c bond is entirely along the axis. In contrast, one of the bonds of the (10, 10) tube is entirely along the circumference; it is not expected to oppose any resistance neither to compression nor to tensile strain. For this reason, nanotube (10, 10) is intuitively the easiest to stretch or to compress, as confirmed by our results in Table II.

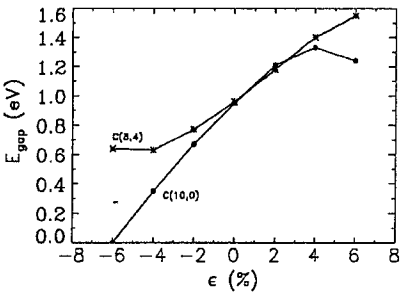

FIG. 3. Band gaps of indicated carbon nanotubes as functions of compression and tensile strain.

We also calculated the in-plane stiffness C for the carbon nanotubes. It is 340, 267, and 272 J/m^2 for (10, 0), (8, 4), and (10, 10), respectively. The in-plane stiffness of these nanotubes exhibited a dependence on their chirality, when the nanotubes are strained along the tube axis (z-direction). Xiao and Liao reported an average in-plane stiffness C of 328 J/m^2 for graphene, using the second-generation Brenner potential in their simulation of carbon nanotubes.[22]

The calculated electronic properties for the unstrained nanotubes basically reproduced the results of Zhao *et al.*[20] for (10, 0) and (8, 4), using the optimal basis sets of the BZW method, which gave converged results for the calculated electronic structure that included the occupied electron states as well as the unoccupied ones near the Fermi level. These tubes were found to be semiconductors. These authors provided plots of the band structures of these tubules.[20] The electron energy bands of carbon nanotube (10, 10) present a semimetallic property as reported in previous publications. Figure 3 shows the nonlinear variation of band gaps of (10, 0) and (8, 4) with strain. For both nanotubes, the band gap decreases with compression strain and increases with tensile strain, for strain values smaller than or equal to 4%. While the band gap for (8, 4) reaches a minimum for a compression strain of 4%, that for (10, 0) exhibits a maximum for a tensile strain of 4%. Our results for the variation of the band gap with strain qualitatively agree with the findings from tight binding[21] but are quantitatively different,[6] particularly in the magnitudes of the band gaps. As apparent in Fig. 3, our results indicate that nanotube (10, 0) become metallic at 6% compression strain. It was noticed that the carbon nanotubes may collapse for large strains,[32,33] a process that we cannot simulate at present using the *ab initio* quantum calculations, because the required computations are beyond our current computation capability. Therefore, the obtained band gaps for large strains may be a theoretical simulation. *A priori*, the general behavior of these band gaps with strain, particularly from values below 4%, is expected on the basis of the increase or decrease of the overlap between atomic sites, for compression or tensile strains, respectively. The consequent broadening or flattening of the bands, respectively, affects the gaps.

A discussion of our results for the elastic properties is partly limited by the dearth of experimental data and by the rather large uncertainty associated with currently available

ones. Indeed, Treacy *et al.*[26] and Wong and coworkers[27] reported average Young's moduli of 1.8 and 1.28 TPa with respective uncertainties of 1.4 and 0.59 TPa. Given these large error margins, the claimed agreement between our results and experimental ones may not have much significance. A comparison with previous theoretical studies is hampered by the differences in the expressions of the Young's modulus for carbon nanotubes as explained by Hernández and coworkers.[10] These authors found 1.22 and 1.24 TPa for the Young's moduli of (10, 0) and (10, 10) respectively. The tight-binding work of these authors, as per their Fig. 3, led to about the same modulus for $(n,0)$ and (n,n) single-walled carbon nanotubes for diameters between 0.75 and 2 nm. This finding is qualitatively different from ours. Lu[9] also found, using the empirical force-constant model, values of 0.975 and 0.972 TPa for (10, 0) and (10, 10), respectively. Our results are clearly different for the three nanotubes under consideration. Our results of 1.47 and 0.726 TPa for nanotubes (10, 0) and (10, 10), respectively, qualitatively agree with the trend in the recent tight-binding work of Zhang *et al.*[28] who found the elastic limit of $(n,0)$ tubes to be about twice that of (n,n) tubes of comparable radius. Another indication of the possible correctness of our findings may reside in the case of graphite. Indeed, the Young's modulus of graphite along the c axis, 0.0365 TPa, is very different from the one in the basal plane, 1.02 TPa.[29]

Due to our utilization of the BZW method, our calculated band gaps are expectedly higher than other theoretical findings known to us. While Reich *et al.*[30] reported a gap of 0.8 eV for nanotube (8, 4), we found 0.96 eV. More importantly, our results clearly show that the variation of the band gap with strain is far from being linear. For nanotubes (10, 0) and (8, 4), the average increase of the band gap per tensile strain under 2% is 0.125 eV. This result is larger than a previously estimated maximum variation[31] of 0.100 eV per percent strain, as is reportedly the case for bulk semiconductor.

In conclusion, this work reported the calculated structural, elastic, and electronic properties of selected, single-wall carbon nanotubes (10, 0), (8, 4), and (10, 10) under uniaxial strain. The results of our *ab initio*, self-consistent, GGA-BZW calculations agreed qualitatively with some findings of the tight binding approach and quantitatively disagreed with them. We found that the radii of these nanotubes do not change under uniaxial strain, up to 6%. We quantified the linear variation of bond lengths with compression and tensile strain and showed the change of the band gap with strain, for semiconducting nanotubes, to be essentially nonlinear. Measurements of elastic limits for $(n,0)$ and (n,n) nanotubes and of the Young's moduli and the in-plane stiffness for graphite qualitatively agree with the trends in our calculated results for the selected single-walled carbon nanotubes.

Recently, we received two preprints regarding the experimental work by S. B. Cronin *et al.* at Harvard University and the Massachusetts Institute of Technology on measurements of uniaxial strain in single-wall carbon nanotubes, utilizing resonance Raman spectra of atomic-force microscope modified SWCNTs. This work entailed bending the nanotubes while holding the ends fixed. Two important comments should be made about this finding. The first one consists of the fact that our calculations did not include a determination of whether or not the nanotubes actually conserve their symmetrical geometry under strain as high as 6%. Cronin *et al.*[32] reported cases where carbon nanotubes broke under strains greater than 1.65%. The second comment stems from an indication, from the work of Cronin *et al.*,[32,33] that the radii of semiconducting SWCNTs do not change under strains between 0.06 and 1.65%. The constancy of the radial breathing mode (RBM) frequency (ω_{RBM}) lead to this conclusion,[32,33] given that the tube diameter $d_t = 248/\omega_{\mathrm{RBM}}$.

ACKNOWLEDGMENTS

This work was funded in part by the National Aeronautics and Space Administration (NASA Award No. NCC 2-1344), the Department of the Navy, Office of Naval Research (ONR, Awards No. N00014-05-1-0009 and No. N00014-04-0587), and the National Science Foundation (NSF Award No. HRD-0000272).

*Corresponding author. Email address: zhao@grant.phys.subr.edu

[1] M. Wilson, K. Kannangara, G. Smith, M. Simmons, and B. Raguse, *Nanotechnology: Basic Science and Emerging Technologies* (Chapman and Hall, Boca Raton, 2002).
[2] C. T. White and J. Mintmire, Nature (London) **394**, 29 (1998).
[3] J. W. Mintmire and C. T. White, Phys. Rev. Lett. **81**, 2506 (1998).
[4] L. Yang, M. P. Anantram, J. Han, and J. P. Lu, Phys. Rev. B **60**, 13 874 (1999).
[5] L. Yang and J. Han, Phys. Rev. Lett. **85**, 154 (2000).
[6] L. Yang, J. Han, M. P. Anantram, and R. Jaffe, Comput. Model. Eng. Sci. **3**, 675 (2002).
[7] M. Ouyang, J. L. Huang, C. L. Cheung, and C. M. Lieber, Science **292**, 702 (2001).
[8] B. I. Yakobson, C. J. Brabec, and J. Bernholc, Phys. Rev. Lett. **76**, 2511 (1996).
[9] J. P. Lu, Phys. Rev. Lett. **79**, 1297 (1997).
[10] E. Hernández, C. Goze, P. Bernier, and A. Rubio, Phys. Rev. Lett. **80**, 4502 (1998).
[11] D. Sanchez-Portal, E. Artacho, J. M. Soler, A. Rubio, and P. Ordejón, Phys. Rev. B **59**, 12 678 (1999).
[12] V. N. Popov, V. E. Van Doren, and M. Balkanski, Phys. Rev. B **61**, 3078 (2000).
[13] J. P. Perdew and W. Yue, Phys. Rev. B **33**, 8800 (1986); J. P. Perdew, *ibid.* **33**, 8822 (1986); J. P. Perdew and A. Zunger, *ibid.* **23**, 5048 (1981).
[14] P. Hohenberg and W. Kohn, Phys. Rev. **136**, B864 (1964).
[15] W. Kohn and L. J. Sham, Phys. Rev. **140**, A1133 (1965).
[16] J. Callaway and N. H. March, in *Solid State Physics*, Vol. 38, edited by H. Ehrenreich, D. Turnbull, and F. Seitz (Academic Press, New York, 1984), p. 135, and references therein.
[17] G. L. Zhao, D. Bagayoko, and T. D. Williams, Phys. Rev. B **60**,

1563 (1999).
[18] D. Bagayoko, G. L. Zhao, J. D. Fan, and J. T. Wang, J. Phys.: Condens. Matter **10**(25), 5645 (1998).
[19] D. Bagayoko and G. L. Zhao, Int. J. Mod. Phys. B **13**(29, 30 & 31), 3767 (1999).
[20] G. L. Zhao, D. Bagayoko, and L. Yang, Phys. Rev. B **69**, 245416 (2004).
[21] M. Dresselhaus, G. Dresselhaus, and P. Ecklund, *Science of Fullerenes and Carbon Nanotubes* (Academic Press, San Diego, 1996); also see C. Kittel, *Introduction to Solid State Physics*, 7th ed. (Wiley, Brisbane, 1996).
[22] T. Xiao and K. Liao, Phys. Rev. B **66**, 153407 (2002).
[23] A. Sears and R. C. Batra, Phys. Rev. B **69**, 235406 (2004).
[24] D. Sanchez-Portal, E. Artacho, J. M. Soler, A. Rubio, and P. Ordejon, Phys. Rev. B **59**, 12 678 (1999).
[25] G. Van Lier, C. Van Alsenoy, V. Van Doren, and P. Geerlings, Chem. Phys. Lett. **326**, 181 (2000).
[26] M. M. J. Treacy, T. W. Ebbesen, and J. M. Gibson, Nature (London) **381**, 678 (1996).
[27] E. W. Wong, P. E. Sheehan, and C. M. Lieber, Science **277**, 1971 (1997).
[28] Peihong Zhang, Paul E. Lammert, and Vincent H. Crespi, Phys. Rev. Lett. **81**, 5346 (1998).
[29] O. L. Blakslee *et al.*, J. Appl. Phys. **41**, 3373 (1970); E. J. Seldin and C. W. Nezbeda, *ibid.* **41**, 3389 (1970).
[30] S. Reich, C. Thomsen, and P. Ordejón, Phys. Rev. B **65**, 155411 (2002).
[31] E. D. Minot, Yuval Yaish, Vera Sazonova, Ji-Yong Park, Markus Brink, and Paul L. McEuen, Phys. Rev. Lett. **90**(15), 156401 (2003).
[32] S. B. Cronin, A. K. Swan, M. S. Unlu, B. B. Goldberg, M. S. Dresselhaus, and M. Tinkham, Phys. Rev. Lett. **93**, 167401 (2004).
[33] S. B. Cronin, A. K. Swan, M. S. Unlu, B. B. Goldberg, M. S. Dresselhaus, and M. Tinkham (unpublished).

Ab-Initio Simulations of the Growth and Structural Properties of Short Carbon Nanobells

G. L. Zhao[1,a], D. Bagayoko[1], and E. G. Wang[2]

[1]Department of Physics, Southern University and A & M College
Baton Rouge, Louisiana 70813, USA
[a] E-mail address: zhao@grant.phys.subr.edu
[2]State Key Laboratory for Surface Physics, Institute of Physics,
Chinese Academy of Sciences, Beijing, 100080, P. R. China

Keywords: carbon nanobells, carbon nanotubes, growth and structural properties of nanobells.

Abstract: We performed ab-initio density functional simulations to study the structural and growth properties of short carbon nanobells. We used a real space approach and the linear combination of atomic orbitals (LCAO) formalism. In the nitrogen-doped carbon nanobells, the nitrogen atoms that are attracted to the open-edge sites of the carbon nanobells play an important role in the growth of the short carbon nanostructures. We present the calculated electronic structure of the short nanobells. The calculated local density of states of the nanobells revealed field emission characteristics that agree with experimental observations.

I. Introduction

The carbon nanostructures present interesting properties with a great potential of applications. Particularly, short carbon nanotubes or carbon nanobells present excellent field-emission properties that have attracted a great interest for applications.[1-8] Experiments demonstrated that the nitrogen-assisted synthesis can grow carbon nanofibers on a large scale.[9-12] Such carbon nanofibers exhibit a "bamboo-like" structure. Distinctively, a great part of the bamboo-like nanofibers consists of short carbon nanobells. Individual nanobells are self-contained and stack one on top of the other to create a long nanofiber. The carbon nanobells may be viewed as short nanotubes such that their lengths are of the same order as their diameters. The electronic structure of the short carbon nanobells is substantially different from that of the pure and long carbon nanotubes because of the quantum effects inherent to their sizes. The nanobells exhibit novel electron field emission properties with a turn-on field of electron emission as low as $0.8 V/\mu m$.[9,13] We performed ab-initio density functional calculations, aiming to understand the growth, structural, and electronic properties of short carbon nanobells.

II. Method

Although the experimental synthesis of carbon nanobells produced samples of various sizes, measurements revealed that the atomic structure of the bamboo-like morphology in thick nanobells is similar to that of the thinner ones.[9] Experiments also revealed that adjacent nanobells do not have a firm contact, but instead the closed end of one nanobell is weakly inserted into the open end of another. Single nanobells can be easily separated from other part of the nanofiber.[10] Hence, our ab-initio calculations will focus on single nanobells. The weak interaction between adjacent carbon nanobells may be included as a perturbation in further studies in modeling the bamboo-like morphology of the nanofibers. We constructed a prototypical

carbon nanobell as a model to simulate the general structure of short carbon nanobells. Fig. 1 presents the calculated images of the electron density distribution of a prototypical carbon nanobell in real space. The prototypical carbon nanobell includes 150 atoms and consists of half of the C240 fullerene with 30 extra atoms on the bell. Its length and diameter are 8.5 and 7.4 $\mathring{A}$, respectively. Although the size of this prototypical carbon nanobell may differ from that of fabricated samples, their fundamental features are similar. These features include the structural properties of the open-edge, the wall, and the closed cap of the nanobells.

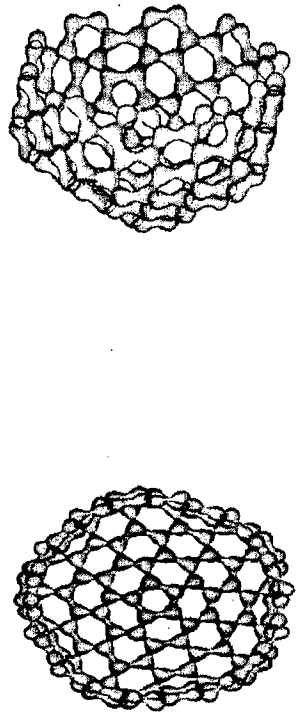

Fig. 1. The calculated images of the electron density distribution in real space for a prototypical carbon nanobell that is viewed from different directions

Our ab-initio calculations are based on the density functional theory of Hohenberg-Kohn and Kohn-Sham.[14,15,16,17,18] In the linear combination of atomic orbitals (LCAO) method, we solved the Kohn-Sham equations self-consistently by employing the Rayleigh-Ritz variational process.[19,20] In the self-consistent calculations for the electronic structure of short CN_x nanobells, we employed an extended basis set that includes atomic orbitals of C(1s2s3s 2p3p) and N(1s2s3s 2p3p). Here C(3s 3p) and N(3s 3p) are extra orbitals that are used to augment the basis set to account for possible charge diffusion and polarization in the short nanobells. The real space approach of the LCAO method enables us to complete the required computations using our SiliconGraphics Origin2000 that is equipped with 2 GB RAM (memory).

III. Results

(A). Relaxed Atomic Structure near the Open-Edge of the Short Carbon Nanobell.

The open-edges of carbon nanobells play an important role in their electronic properties. The structure near the open edge of the carbon nanobell is different from that in the inner wall and the closed cap. We performed total energy minimization to identify the atomic structure near the open-edge of the prototypical carbon nanobell. The calculated C-C bond length on the first atomic ring at the open-edge of the carbon nanobell is $1.37\,\mathring{A}$, which is much shorter than the C-C bond length of $1.415\,\mathring{A}$ in the inner atomic rings of the bell. This reduction of the C-C bond length for the carbon atoms at the open-edge sites is a result of the reduction in coordination number. The calculated bond length of the carbon atoms on the first atomic ring to the carbon atoms on the second ring is $1.40\,\mathring{A}$, which is not much different from that

in the inner rings, away from the open-edge of the nanobell. This result indicates that the effect of further relaxation of the third atomic ring and inner rings would be insignificant.

(B). A Possible Growth Mechanism of Carbon Nanobells. The growth mechanism of the carbon nanobells remains a difficult problem. There are probably two major growth models.[1] The first one assumes that the carbon atoms are added at the open-ends of the nanobells. [1,11] The second one involves the C_2 absorption process that is assisted by the pentagonal defects on the closed caps.[1] Although both models are very interesting, we have technical difficulties using density functional computations to simulate the second growth model. We successfully performed local density functional computations to test the first growth mechanism. Because of the active dangling bonds of carbon atoms at the open-edge of nanobells, there is a high possibility that carbon atoms can be attracted to these sites for growth to occur. We calculated the total energies in the following two cases. In the first case, a ring of 20 carbon atoms attaches to the open-edge of the carbon nanobell at a bond-length of 1.415 $\mathring{A}$. In the second case, these 20 carbon atoms are free. The calculated total energy in case I is substantially lower than the corresponding value in case II. The total energy difference, which may also be defined as the cohesive energy of the carbon atoms in the first growth model, is 4.7 eV/atom. In this growth model, see Fig. 1, C_2 dimers are absorbed at the active dangling bond sites at the open end of the carbon nanobell. A C_2 dimer that deposits on the open-edge of the bell forms one covalent bond on the same atomic ring. Each of the C atoms also forms one covalent bond with the C atom of the next atomic ring and remains an active dangling bond towards the open-space. This grow model is consistent with previous analysis of experimental results.[11,13, 21] Although we cannot rule out the second growth model (growth on the closed cap of carbon nanobells), our calculations presented a clear evidence that the first growth mechanism is highly possible.

(C). Nitrogen-Doped Carbon Nanobell. Experimental results indicated that the growth of the short carbon nanobells is highly dependent on the nitrogen concentration in the gas mixture during the synthesis.[9,10] Without nitrogen atoms in the growth gas mixture under the same conditions, long and pure carbon nanotubes, without the "bamboo-like" morphology, are produced. However, it was not clear why the nitrogen atoms could turn the growth of the would-be long carbon nanotubes into that of short carbon nanobells. We performed total energy calculations to study the nitrogen-doped carbon nanobells (CN_x nanobells). Since nitrogen atoms can also form the planar sp^2-hybrid,[22] we studied the substitutional doping of nitrogen atoms in the CN_x nanobells. The substitutional doping of nitrogen atoms in CN_x nanobells was also proposed from the analysis of experimental results.[13]

We first replaced carbon atoms with nitrogen atoms at the open-edge of the prototypical nanobell. We compared the total energies in the two cases. In the first case, computations are carried out for the pristine carbon nanobell in the presence of ten free atoms of nitrogen. In the second case, ten nitrogen atoms replace ten carbon atoms on the open-edge and the substitutionally N-doped nanobell is in the presence of ten free atoms of carbon. The calculated total energy in the second case is lower than that in the first case by an amount of 0.5 eV per atom, without relaxing the structure. We then performed total energy calculations and identified the atomic positions of the relaxed structure of the nitrogen-doped nanobell from the total energy minimization. The calculated C-N bond length in the first atomic ring at the

open-edge of the nanobell is 1.376 $\mathring{A}$. The bond-length, from the nitrogen atoms of the first atomic ring to the carbon atoms of the second atomic ring, is 1.377 $\mathring{A}$. They are close to the length of the partially double C-N bond (1.352 $\mathring{A}$) in heterocyclic systems.[23] The C-C bond length from the first atomic ring to the second ring is 1.397 $\mathring{A}$. The total energy of the nitrogen-doped nanobell, in the relaxed structure, is lower than that of the undoped one by 0.72 eV per atom.

We also studied the substitutional doping with nitrogen atoms (for carbon atoms) in the wall (away from the open-edge and the closed cap) of the prototypical carbon nanobell. We used the same computation procedure as discussed above. The calculated total energy of the N-doped nanobell, at the wall position, is much higher than that of the undoped bell by an amount of 5 eV per atom. This result indicates that the substitutional doping with nitrogen in the wall of carbon nanobells is not energetically favored.

These calculated results for the nitrogen-doped nanobells in the prototypical model thus indicate that the dopant nitrogen atoms prefer to stay at the open edge of the nanobell as opposed to being in the wall (i.e. lower rings) of the nanobell. Once there are enough nitrogen atoms on the open edge of the nanobell, carbon atoms cannot attach to the open-edge of the CN_x nanobell. Such an attachment will result in nitrogen atoms being in inner rings other than that at the open-edge, resulting in a configuration that is not favored energetically. Consequently, nitrogen atoms act as the stopper of the growth of the carbon nanobell. This growth mechanism for the nitrogen-doped carbon nanobells and the effect of the nitrogen atoms in the growth process agree with the observations from experiments.[9,10,11,13]

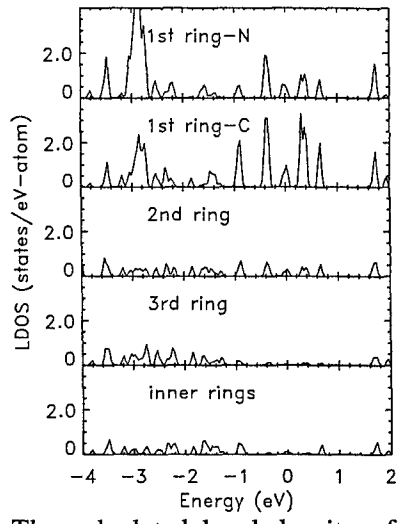

Fig. 2. The calculated local density of states of electrons of a nitrogen-doped carbon nanobell. The 1st ring-N and –C refer to the nitrogen and carbon atoms on the first atomic ring at the open-edge of the nanobell. The 2nd and 3rd rings refer to the second and third atomic rings near the open-edge. The inner rings refer to the atomic sites away from the open-edge, including the closed cap. The Fermi level is at 0.0 eV.

We present the calculated local density of states (LDOS) of the CN_x nanobell in Fig. 2. The dopant nitrogen atoms stay at the open-edge sites in the prototypical nanobell. The LDOS from the nitrogen and carbon atoms on the first atomic ring at the open-edge of the nanobell are shown in the first and the second panels of Fig. 2, respectively. There is no N atom on other atomic rings away from the open-edge of the nanobell. Fig. 2 clearly shows that the N and C atoms on the first atomic ring at the open-edge of the nanobell have the dominant contribution to the electronic states around the Fermi level. The LDOS at the Fermi level, from the N and C atoms on the first atomic ring at the open-edge, are 0.56 and 0.71 states per eV per atom, respectively. The contribution, from the second atomic ring near the open-edge, to the LDOS at the Fermi level is 0.23 states per eV per atom. The third atomic ring and the inner rings, that include the closed cap, have a much smaller contribution to LDOS at the Fermi level, at

about 0.08 states per eV per atom. Thus, electrons will be emitted from the atomic sites near the open-edge of the nanobell in field-emission experiments. The LDOS of Fig. 2 exhibit a nearly metallic behavior. The real nanobell samples in experimental studies mostly involve multilayers of graphite sheets and the nanobells stacked one on top of the other. The weak interactions between graphite layers in these nanobells and that between the bells may further broaden the electronic energy levels. Consequently, a metallic behavior may be observable in the measurements of the electronic structure of N-doped nanobells.

IV. Conclusion

In conclusion, we performed ab-initio density functional calculations to simulate the growth, structural, and electronic properties of prototypical carbon nanobells. In the nitrogen-doped carbon nanobells, nitrogen atoms that are attracted to the open-edge of the nanobells may play a role of stopper of the growth of the nanostructures. The calculated local densities of states of the CN_x nanobells indicate that electrons are most likely emitted from the atomic sites near the open-edge of the carbon nanobell in field-emission experiments. This result agrees with experimental observations.

Acknowledgements: This work was funded in part by the US Department of the Navy, Office of Naval Research (ONR Award No: N00014-05-1-0009) and by US NASA (Award No. NCC 2-1344).

References

[1] M. S. Dresselhaus, G. Dresselhaus, and P. C. Eklund: Science of Fullerenes and Carbon Nanotubes, (Academic Press, New York, 1996).
[2] Walt A. de Heer, A. Châtelain, D. Ugarte: Science, Vol. **270** (1995), 1179.
[3] A. G. Rinzler, et al: Science, Vol. **269** (1995), 1550.
[4] Q. H. Wang, et al: Appl. Phys. Lett. Vol. **70** (1997), 3308
[5] Q. H. Wang, et al: Appl. Phys. Lett. Vol. **72** (1998), 2912.
[6] Y. Chen, et al: Appl. Phys. Lett. Vol. **73** (1998), 2119.
[7] K. A. Dean and B. R. Chalamala: Appl. Phys. Lett. Vol. **76** (2000), 375.
[8] J. M. Bonard, et al: Phys. Rev. Lett. Vol. **81** (1998), 1441.
[9] X. Ma, E. Wang, W. Zhou, D. A. Jefferson, J. Chen, S. Deng, N. Xu, and J. Yuan: Appl. Phys. Lett. Vol. **75** (1999), 3105.
[10] X. Ma, E. G. Wang, R. D. Tilley, D. A. Jefferson, and W. Zhou: Appl. Phys. Lett. Vol. **77** (2000), 4136.
[11] X. Ma, and E. G. Wang: Appl. Phys. Lett. Vol. **78** (2001), 978.
[12] E. G. Wang, et al: Carbon Vol. 41 (2003), p.1827.
[13] D. Y. Zhong , S. Liu, G. Y. Zhang, E. G. Wang: J. of Appl. Phys. Vol. **89** (2001), 5939.
[14] P. Hohenberg and W. Kohn: *Phys. Rev.* Vol. **136** (1964), B864; W. Kohn and L. J. Sham: *Phys. Rev.* Vol. **140** (1965), A1133.
[15] G. L. Zhao, D. Bagayoko, and L. Yang: Phys. Rev. B vol. Vol. **69** (2004), 245416.
[16] J. Callaway and N. H. March: *Solid State Physics*, vol. 38, Edited by H. Ehrenreich, D. Turnbull, and D. Seitz, (Academic Press, New York, 1984), p.135.
[17] G. L. Zhao, D. Bagayoko, and E. G. Wang: Modern Physics Letters B, vol. 17 (2003), 375.
[18] D. Bagayoko, G. L. Zhao, J. D. Fan, and J. T. Wang: *Journal of Physics: Condensed Matter*, Vol. **10** , (1998), 5645.
[19] S. G. Mikhlin: *The Numerical Performance of Variational Methods*, (Wolters-Noordhoff Publishing, 1971), ch.1, 2, & 7.
[20] S. H. Gould: *Variational Methods for Eigenvalue Problems*, (University of Toronto Press, 1957), ch. 2.
[21] J. Gavillet, A. Loiseau, C. Journet, F. Willaime, F. Daucastelle, and J. C. Charlier: Phys. Rev. Lett. Vol. **87** (2001), article #275504.
[22] W. A. Harrison: Electronic Structure and the Properties of Solids, (W. H. Freeman and Company, San Francisco, 1980), p. 91.
[23] CRC Handbook of Chemistry and Physics, Edited by R. C. Weast. D. R. Lied, M. J. Astle, and W. H. Beyer, (CRC Press, Boca Raton, Florida, 1990), p. F-188.

A Universal Relation between the Densities of States near Van Hove Singularities and the Effective Electron Masses in 1-Dimensional Semiconductors

G. L. Zhao* and D. Bagayoko

Department of Physics, Southern University and A & M College
Baton Rouge, Louisiana 70813, USA
* E-mail address: zhao@grant.phys.subr.edu

Keywords: nanotubes, 1-D semiconductors, electron masses, van Hove singularities.

Abstract. We present a universal relation between the densities of states near Van Hove singularities and the effective electron masses in 1-dimensional (1-D) semiconductors. The relation can be utilized as a new method to determine the effective masses of charge carriers of 1-D semiconductors in theoretical calculations and in experimental measurements. The calculated results, utilizing the relation for 1-D single-walled carbon nanotubes (SWCNTs), agree well with that of the conventional calculations when both approaches utilize the outputs of ab-initio density functional computations.

I. Introduction.

One-dimensional (1-D) materials, such as carbon nanotubes (CNTs), have emerged as attractive materials for applications in molecular-scale electronics.[i,ii] The electronic properties of 1-D CNTs have been extensively studied in recent years using various experimental tools and theoretical calculations.[ii,iii,iv] Particularly, scanning tunneling microscopy (STM) is a favorable tool for measuring atomic structures, density of states (DOS) of electrons, Van Hove singularities, and energy band gaps. However, there are some other physical quantities that require further studies. One of them is the effective mass of charge carriers (electrons or holes), an important physical quantity that characterizes the electronic transport properties of materials. Here, we present a universal relation between the densities of states of electrons near Van Hove singularities and effective electron masses in 1-D materials. This relation can be used as a new method to determine the effective masses of charge carriers in any 1-D semiconductors.

II. Densities of States and Effective Masses in 1-D Materials.

The electron density of states (DOS) per unit cell, G(ε), of a 1-D material can be calculated by the following expression.[v]

$$G(\varepsilon) = \frac{L}{2\pi} \sum_{(\varepsilon_{ik}=\varepsilon)} \frac{1}{\left|\frac{d\varepsilon_{ik}}{dk}\right|} \qquad (1)$$

where ε_{ik} is the energy of the i-th electron band at point k in the irreducible Brillouin zone; and L is the length of the unit-cell.

At an extremal point of an electron energy band, the first derivative of the band energy with respect to the wave vector k is zero, that is $d\varepsilon_{ik}/dk = 0$. A Van Hove singularity occurs at this point. We can then approximate the band dispersion as a parabolic

expression in the neighborhood of the extremal point that particularly includes the top or the bottom of an energy band,

$$\varepsilon_{ik} = \varepsilon_i \pm a_i (k - k_i)^2 \qquad (2)$$

where k_i and ε_i are the location and the band energy at the extremal point, respectively. Here $a_i > 0$. When the second derivative of the band energy with respect to the wave vector k is also zero, the effective mass of the charge carrier near the Van Hove singularity is not defined. Therefore, we do not discuss this case further in this article.

We can then calculate the electron density of states per unit cell near the Van Hove singularity as follows

$$D(\varepsilon) = G(\varepsilon)/L = \frac{1}{4\pi} \sum_{(\varepsilon_{ik}=\varepsilon)} \frac{1}{\sqrt{a_i}\sqrt{|\varepsilon_{ik} - \varepsilon_i|}} \qquad (3)$$

where $D(\varepsilon)$ is a reduced density of states, which does not depend on the length of the unit cell.

We can calculate the effective mass of charge carriers using the electron energy band dispersion,

$$m_i^* = \frac{\hbar^2}{\left|\frac{d^2\varepsilon_{ik}}{dk^2}\right|} = \frac{\hbar^2}{2a_i} \qquad (4)$$

where m_i^* is the effective mass of charge carriers (electrons or holes) near the extremal point of the i-th band.

III. A Relation between DOS and m_i^* in 1-D Materials.

(A). Case of single bands. We first consider the case of a single band. The dispersion of a single electron band of a 1-D material near its Van Hove singularity can be written as

$$\varepsilon_{1k} = \varepsilon_1 \pm a_1 (k - k_1)^2 \qquad (5)$$

We obtain the density of states and the effective electron mass of this single band as $D_1(\varepsilon) = \frac{1}{4\pi} \frac{1}{\sqrt{a_1}\sqrt{|\varepsilon - \varepsilon_1|}}$ and

$m_1 = \frac{\hbar^2}{2a_1}$.

If a second single band of the same material or another 1-D material near the Van Hove singularity is,

$$\varepsilon_{2k} = \varepsilon_2 \pm a_2 (k - k_2)^2 \qquad (6)$$

We then have the density of states and the effective mass of this second single band as $D_2(\varepsilon) = \frac{1}{4\pi} \frac{1}{\sqrt{a_2}\sqrt{|\varepsilon - \varepsilon_2|}}$ and

$m_2 = \frac{\hbar^2}{2a_2}$.

Using the above equations, we identify the following relation,

$$\frac{m_1}{m_2} = \frac{a_2}{a_1} = \left[\frac{D_1(\varepsilon + \varepsilon_0)}{D_2(\varepsilon + \varepsilon_2)}\right]^2 \qquad (7)$$

The above relation does not depend on the energy. Once the effective mass for a single electron band of a 1-D material is known, we can then take it as a reference. The effective masses of charge carriers (electrons or holes) for any other single bands of other 1-D materials can be calculated using the above relation and corresponding densities of states near Van Hove singularities.

(B). Case of bands that are degenerate at an extremal point, but are not degenerate elsewhere. If two bands are degenerate at an extremal k-point, but are not degenerate elsewhere, we may assume the dispersions of the two as,

$$\varepsilon_k^{(i)} = \varepsilon_2 \pm b^{(i)} (k - k_2)^2 \qquad (8)$$

where i=1 or 2 for the two bands, respectively. We may take a single band of a 1-D material as a reference, for

which the band dispersion follows Eq. (5). The density of states and the effective mass of this single band has been discussed in the previous section. We then identify the relation as,

$$\frac{\overline{m}_2^*}{m_1} = \left[\frac{D_2(\varepsilon+\varepsilon_1)}{2D_1(\varepsilon+\varepsilon_0)}\right]^2 \qquad (9)$$

where $\overline{m}_2^*$ and $D_2(\varepsilon)$ are the average effective mass and the density of states of the doubly degenerate bands, respectively.

$$\overline{m}_2^* = \frac{1}{4}\left[\sqrt{m_2^{(1)}} + \sqrt{m_2^{(2)}}\right]^2 \qquad (10)$$

where $m_2^{(1)} = \dfrac{\hbar^2}{2b_1}$ and $m_2^{(2)} = \dfrac{\hbar^2}{2b_2}$.

The above discussions can also be extended to three or more energy bands that are degenerate at an extremal point, but are not degenerate elsewhere.

IV. Applications.

Although there is a wealth of experimental results regarding the density of states of electrons in single-walled carbon nanotubes (SWCNTs),[ii,iii] the study of the effective masses of the charge carriers in these materials is far from complete. As a test case of the new method to study the effective masses of the charge carriers in 1-D materials, we applied Eq.(7) or (9) to some SWCNTs. We list some of the results in Table 1, where m_0 is the free electron mass. $E_v^{(1)}$ in Table 1 refers to the first valence band near the Fermi level (E_F), whereas $E_c^{(1)}$ refers to the first conduction bands from E_F. Em is the energy (in eV) of the top of a valence band or the bottom of a conduction band near its Van Hove singularity. The energy of the top of the first valence band ($E_v^{(1)}$) has been chosen to be zero in Table 1. "Deg" refers to the degeneracy of the bands. Dm (in states/eV) is the peak value of the density of states at the Van Hove singularity; it was used to calculate the effective mass $\overline{m}^*$ using the universal relation, Eq.(7) or (9). We utilized the effective mass of charge carriers of SWCNT (10, 0) at $E_v^{(1)}$ as the single reference for the calculations of the effective masses ($\overline{m}^*$) of other SWCNTs. As a comparison, we also calculated the effective mass m* using the results of the conventional method for which we utilized the ab-initio electronic structure calculations. We performed self-consistent, ab-initio density functional calculations to obtain the electronic structure of the SWCNTs, using a linear combination of atomic orbital (LCAO) method.[6-10] Particularly, the ab-initio calculations for the electronic structure of nonsymmorphic SWCNTs (8, 4) and (10, 5) are very difficult tasks, since there are 112 and 140 atoms in their tubule unit cells, respectively. The calculated results of the effective masses $\overline{m}^*$ of the charge carriers in SWCNTs utilizing the universal relation Eq. (7) or (9) agree very well with those from the conventional method of ab-initio electronic structure calculations, as demonstrated in Table 1.

Acknowledgments: the work was funded in part by the US Department of the Navy, Office of Naval Research (ONR Award No: N00014-05-1-0009) and by US NASA (Award No. NCC 2-1344).

Table 1. The calculated effective masses of charge carriers in various 1-D SWCNTs, where m* is the calculated effective mass from ab-initio density functional computations; $\overline{m}^*$ is obtained using the universal relation Eq. (7) or (9); and Dm is the peak value of the density of states near Van Hove singularity.

Band	E_m (eV)	Deg	m*(ab-initio) (m_0)	D_m (states/eV)	$\overline{m}^*$ (Eq. 7 & 9) (m_0)
SWCNT (10, 0)					
$E_v^{(1)}$	0.0	2	0.10	0.73	0.10
$E_c^{(1)}$	0.95	2	0.10	0.72	0.10
SWCNT (13, 0)					
$E_v^{(1)}$	0.0	2	0.09	0.66	0.08
$E_c^{(1)}$	0.75	2	0.09	0.66	0.08
SWCNT (17, 0)					
$E_v^{(1)}$	0.0	2	0.11	0.73	0.10
$E_c^{(1)}$	0.54	2	0.11	0.72	0.10
SWCNT (22, 0)					
$E_v^{(1)}$	0.0	2	0.057	0.51	0.05
$E_c^{(1)}$	0.44	2	0.056	0.51	0.05
SWCNT (8, 4)					
$E_v^{(1,2)}$	0.0		0.13	0.76	0.11
$E_c^{(1,2)}$	0.96		0.13	0.76	0.11
SWCNT (10, 5)					
$E_v^{(1,2)}$	0.0		0.11	0.79	0.12
$E_c^{(1,2)}$	0.74		0.11	0.79	0.12

[i] D. Voss: Mit's Technology Review, Vol. 102 (1999), 55.

[ii] M. S. Dresselhau, G. Dresselhaus , and P. C. Eklund: Science of Fullerenes and Carbon Nanotubes, (Academic Press, New York, 1996), Ch. 19

[iii] There are many publications on experimental studies of carbon nanotubes. Some of them include, M. Bockrath, et al: Science, Vol. 291 (2001), 283; M. Ouyan, et al: Science, Vol. 291 (2001), 97; T. W. Odom, et al : J. Phys. Chem. B Vol. 104 (2000), 2794; J W G Wilder, et al: Nature, Vol. 391 (1998), 59; P. Kim, et al: Phys. Rev. Lett. Vol. 82 (1999), 1225

[iv] Some of the theoretical studies of carbon nanotubes include, J W Mintmire, B I Dunlap, and C T White: Phys. Rev. Lett. Vol. 68 (1992), 631; R. Saito et al: Appl. Phys. Lett. Vol. 60 (1992), 2204; N. Hamada et al: Phys. Rev. Lett. Vol. 68 (1992), 1579; C T White and J W Mintmire: Nature, Vol. 394 (1998), 29; L. Yang and J. Han: Phys. Rev. Lett. Vol. 85 (2000) , 154

[v] J. Callaway: Quantum Theory of the Solid State, Student Edition, (Academic Press, New York, 1976), Ch. 4.

[vi] B. N. Harmon et al: Phys. Rev. B Vol. 25 (1982), 1109.

[vii] D. Bagayoko et al: J. Physics: Condensed Matter, Vol. 10 (1998), 5645.

[viii] G. L. Zhao, D. Bagayoko, and T. D. Williams: *Physical Review B* Vol. **60** (1999), 1563.

[ix] G. L. Zhao, D. Bagayoko, and E. G. Wang: Modern Physics Letters B, vol. 17 (2003), 375.

[x] G. L. Zhao, D. Bagayoko, and L. Yang: Phys. Rev. B Vol. **69** (2004), 245416.

Accepted for publication in the Proceedings of the 2005 National Conference of the National Society of Black Physicists (NSBP).

Local Density Functional Description of Electronic Properties of Wurtzite Zinc Oxide (w-ZnO)

D. Bagayoko, G. L. Zhao, and L. Franklin
Department of Physics
Southern University and A&M College
Baton Rouge, Louisiana 70813, USA

Contact information for the corresponding author: Diola Bagayoko, P. O. Box 11776, Southern University and A&M College, Baton Rouge, Louisiana 70813, USA; Telephone: 001-225-771-2730; Fax: 001-225-771-4341; E-mail: Bagayoko@aol.com

Abstract

We report calculated, electronic properties of wurtzite zinc oxide (w-ZnO). Unlike many previous theoretical works, our linear combination of atomic orbital (LCAO) calculations, implemented following the Bagayoko, Zhao, and Williams (BZW) method, employed a local density approximation (LDA) potential to obtain band gaps and other results in agreement with experiments. We discuss the band structures, the calculated direct band gap (3.2 to 3.3 eV), and the electron effective mass (0.25 to 0.26 m_0).

PACS Numbers 71.20.Nr, 71.15.Ap, 71.15.Mb

I. Introduction and Motivations

Nowotny et al [1] and Thomas [2] provided some of the earliest experimental data on wurtzite zinc oxide (w-ZnO), the former on the lattice parameters and the latter on the band gap. A representative set of measurements of the band gap of bulk w-ZnO shows a robust agreement on its low temperature value of 3.44 ± 0.06 eV. [1-7] This range, i.e., ± 0.06 eV, is much larger than experimental uncertainties; it simply reflects differences that a traceable to those of actual lattice constants, measurement techniques and temperatures, and other factors. Some of these factors (impurities, defects) are associated with the growth conditions of the samples. Srikant and Clarke [8] appear to have settled the debate on the room temperature band gap of w-ZnO. They utilized different measurement techniques to arrive at a value of 3.30 eV. These techniques included reflection and transmission absorption, ellipsometric spectroscopy, Fourier transform infrared (FTIR) spectroscopy, and photoluminescence. This multitude of measurement techniques avoided limitations reported to afflict some previous investigations that reported a room temperature band gap of bulk w-ZnO 0.1 and 0.2 eV below the currently accepted value of 3.30 eV. Other groups reported photoemission [9-11] results for the band structure, the electrons effective mass [12] and the bulk modulus [13].

Several groups [14-20] have reported measured band gaps for films of w-ZnO grown by a variety of techniques. These growth methods included spray pyrolisis [14], pulsed laser deposition [16,18], cathodic electrodeposition in aqueous solutions [17], ion layer gas reaction (ILGAR) and rf magnetron sputtering [19], and plasma enhanced chemical vapor

deposition (PECVO). [20] Li and Coworkers [20] discussed the variation of the lattice parameters of films with changes in growth temperatures. They also noted that despites these variations, the lattice parameters (a and c) of the wurtzite films are within $3.4x10^{-3}$ Angstroms from the corresponding values for the bulk material. The reported band gaps for the films are within the range of -0.14 to +0.06 from 3.44 eV. Studenikin et al [14] found a gap of 3.30 eV, after annealing at 400 C, for all their films grown by spray pyrolisis. This result was confirmed by Pauporté and Lincot [17] for films grown by catholic electrodeposition in aqueous solutions. The band gap of their films as deposited was 3.5 eV. These authors [17] noted that growth conditions affect the gap. In particular, the presence of nitrate or perchlorate ions is reported to lead to a band gap of 3.30 eV. Using both transmission and photoluminescence techniques, Muth et al. obtained band gaps of 3.40 eV and 3.45 eV at 295 K and 77 K, respectively. Within the understandable differences due to growth stress, thermal expansion mismatch, and impurities [8], the above band gaps for w-ZnO films are comparable to those for high quality bulk w-ZnO samples.

In contrast to the above agreement between experiments, theoretical calculations reported values of the band gap that cover a wide spectrum and mostly disagree with measurements. The Hartree Fock (HF) calculations [21-24] led to band gaps above 11 eV, more than three times the measured value. When some correlation effects are taken into account, the modified HF calculations of Jaffe et al [21] produced a gap of 8.61 eV. Empirical pseudopotential [25] and empirical KKR [26] calculations predictably led to 3.5 and 3.30 eV, respectively. These values are close to the experimental gap of 3.44 eV. The fitting involved in these empirical approaches can adjust some parameters so as to reproduce the experimental band gap. Local density approximations (LDA) potentials, depending on the computational methods [23, 27-33], led to values between 0.23 eV and 2.26 eV for the band gap of w-ZnO. Table 1, further below, identifies some of the various methods and applicable lattice parameters. The computational approaches include the pseudopotential (PP), the augmented plane wave (APW), the full-potential linearized augmented plane wave (FLAPW), and the linearized muffin-tin orbital (LMTO) methods. The Green function and screened coulomb approximations (GWA) calculations did not totally resolve the above failure of ab-initio calculations to obtain the measured band gap of w-ZnO. The GWA work of Oshikiri and Aryasetiawan [31], for two different sets of lattice constants, obtained 4.28 (4.06) and 3.45 (3.63) eV respectively, with the values between parentheses resulting from using additional higher energy product basis for improved accuracy. The GWA calculations of Usuda et al [30] obtained a gap of 2.44 eV with both the LMTO and LAPW methods. This value is 1 eV below the measured value of 3.44 eV.

The gross disagreement between ab-initio calculations and experiment, as far as the band gap is concerned, basically precludes an extensive discussion of calculated electron effective masses, inasmuch as the latter are determined by the curvature of the band in the immediate vicinity of the lowest energy in the conduction band. Indeed, difficulties responsible for the disagreement on the gap are also expected to affect not just the location of the lowest energy in the conduction band but also the curvature of said band. With the above understanding, we note that Oshikiri et al [34] reported quasiparticle (and

LDA) effective masses of 0.25 (0.21), 0.25 (0.21), and 0.21 (0.18) m_0 in the k_x, k_y, and k_z directions respectively, where the values between parentheses resulted from their LDA calculations. These results were obtained for experimental lattice constants of 3.24961 Å , 5.20653 Å and u parameter of 0.345. Lambrecht et al. [33] noted that their calculated values of 0.23 m_0 and 0.21 m_0, in the parallel and perpendicular directions, are likely to be underestimates. Xu and Ching [35] reported 0.37, 0.28, and 0.32 m_0 in the Γ-K, Γ-A, and Γ-M directions in the Brillouin zone, for lattice constants given in Table 1. These authors utilized the orthogonalized LCAO formalism and employed a local density potential plus additional exchange derived with Wigner's interpolation. The 1966 measurements by Baer [12] found the electron effective mass for w-ZnO to be 0.24 $\pm$ 0.02 m_0. The above LDA results for the electron effective mass are uniformly lower than this experimental value.

The above overview of previous theoretical results, with the general disagreement between calculations, on the one hand, and between calculations and the firmly established experimental data, on the other hand, provides the motivation for this work. The wide spread of the LDA results for the band gap of w-ZnO, from 0.23 to 2.26 eV, suggests that limitations other than those genuinely attributable to the potential affected these results. Since 1998, Bagayoko, Zhao, and Williams have introduced a computational method [36-39] that clearly showed that *LDA potentials are no longer known to lead to woeful underestimates of the band gap of semiconductors.* Indeed, using the Rayleigh theorem, these authors introduced a new form of convergence for variational computations that utilize a basis set. The need to seek methodically [36-37] a basis set whose size is converged [i.e., the optimal basis set] vis a vis the description of the *occupied* states, they argued, straightforwardly arises from (a) the use of *only* the wave functions of the *occupied states* to construct the charge density, the potential, and the Hamiltonian in the iterative process and (b) the Rayleigh theorem that asserts the possible, continuing lowering of some unoccupied energies or bands when basis sets larger than the optimal one are utilized. This extra-lowering of some unoccupied energies, even though the physics (i.e., the Hamiltonian) is no longer changing, was identified as a basis set and variational effect that has afflicted most of the previous calculations, including those utilizing the generalized gradient approximation (GGA) of density functional theory (DFT) [40-41] and the GWA approximation [42]. Hence, the clear motivation of this work is to utilize properly, as per the BZW method, a local density potential to describe the electronic and related properties of w-ZnO. In the remaining of this article, we briefly present our method and discuss our results, which are basically in agreement with experiment, particularly as compared to previous, theoretical ones.

II. Method

Our computational method has been extensively described in previous publications [36-39]. It is characterized by the use of a local density approximation (LDA) potential [43] as parameterized by Vosko et al [44], the well-known linear combination of Gaussian orbitals (LCGO), and the rigorous application of the BZW method in carrying out the calculations. We utilized a program package developed and refined over decades [45-46].

Our calculations are non-relativistic and are performed at zero temperature. They commence with the LCAO, self-consistent calculations of the electronic energy levels of the atomic or ionic species that are present in the system under study. For wurtzite ZnO, these species are Zn (Zn^{2+}) and O (O^{2-}). Specifically, the calculations for the neutral atoms are utilized in preliminary investigations of the solid state. The output of the preliminary calculations is employed to compute ionic charges, if any, in the solid. We found zinc and oxygen elements, in the solid, to be closer to Zn^{2+} and O^{2-} than to neutral Zn and O or Zn^{+1} and O^{1-}. Consequently, ab-initio calculations were performed for Zn^{2+} and O^{2-} in order to obtain the "atomic" basis sets to be employed in the actual solid state calculations.

These self-consistent, solid state calculations, as per the BZW method, started with the minimal basis (MB) set, i.e., the one just enough to account for all the electrons in the system. Calculation II utilized a basis set comprised of the MB set plus orbital(s) representing the next excited level(s) in the ionic (or atomic) species in the system. The occupied energies from Calculations I and II were compared numerically and graphically. As is generally the case, they were different. Hence, Calculation III was performed with a basis set including that of Calculation II as augmented with orbitals representing the next excited levels of the ionic species in the system, i.e., Zn^{2+} and O^{2-}. As discussed below, the occupied energies from Calculations II and III are the same, within computational uncertainties. Hence, the basis set of Calculation II is our optimal basis set, i.e., the one utilized for all results reported here. If the Rayleigh theorem did not apply and if the wave functions of the occupied states were not the only ones utilized in the interactive process to construct the charge density and the Hamiltonian, then the results of Calculation III, with sinking unoccupied bands, would have been the physical answer on the account of basis set completeness considerations. The actual size of the basis set naturally depends on the types of functions, with plane wave approaches entailing many more basis functions than those utilizing exponential or Gaussian functions.

Computational details germane to the replication of our work follow. ZnO (or zincite) possesses a hexagonal lattice in the space group C^4_{6v}. There are four atoms per unit cell in the $(2b)^{47}$ positions as follows: Zn: (0, 0, 0), (1/3, 2/3, 1/2); O: (0, 0, u), (1/3, 2/3, 1/2 + u). The self-consistent computations were performed for different sets of lattice parameters as shown in Table 1. For a given calculation, we employed a mesh of 24 k-points, with proper weights, in the irreducible Brillouin zone. Our criterion for self-consistency rested on the convergence of the potential to a difference around 10^{-5} between two consecutive iterations. Approximately 60 iterations were needed to reach self-consistency. The computational error for the valence charge was about 0.0002 for 52 electrons. For the implementation of the BZW method, our first self-consistent calculation utilized the atomic orbitals of Zn^{2+}(1s2s3s4s2p3p3d) and O^{2-}(1s2s2p). Calculation II included the (4p) orbital on zinc while Calculation III further added the 3p orbital on Oxygen. The comparison of the occupied states from Calculation II and III showed that the convergence of the size of the basis set, vis a vis the description of the *occupied* states, was reached with Calculation II. The basis set of this calculation, the optimal basis set, was employed for the results discussed below.

III. Results

Some of our calculated band structures are shown in Figures 1 and 2. Figure 1 illustrates the dramatic differences between our results and those or previous LDA and other calculations. Essentially, there are no major differences between our calculated occupied bands and some previously reported ones. For the unoccupied bands, however, our results are distinctively far those of previous calculations. In Figure 1, the lowest unoccupied energy at the Γ point is shifted downward by approximately 2.2 eV as compared to its value obtained with the optimal basis set. Clearly, the differences between the low energy conduction bands from calculation II and III are far from those expected from a rigid shift. Hence, they cannot be corrected with simplistic "scissors" operations.

The above differences between our calculated conduction bands and those in previous reports explain the reason our calculated band gaps of 3.2 and 3.278 eV, at lattice constants specified in Table 1 and Figures 1 and 2, are very close to experimentally measured values. The differences between our results from the calculation at the experimental lattice constants in Figure 2 and the one just below it, in Table 1, are mainly due to the difference in the value of u, given that the lattice parameters are not far apart. Schröer and coworkers found a similar situation in their LMTO and GWA calculations. [27] The value of u, understandably, strongly influences that of the band gap.

Our calculated, total (DOS) and partial density of states (pDOS) in Figures 3 and 4 naturally reflect the differences discussed above for the electronic energy bands. In particular, the location of the lowest conduction bands with respect to the Fermi energy in these figures is drastically different from that in most of the previous theoretical investigations. The inset in Figure 3 illustrates our concept of a practical band gap. [37] Essentially, due to instrumental sensitivity, analysis techniques, and related uncertainties, an experimental work could find values of the band gap from the theoretical minimum of 3.278 to close to 4.0 eV. This possibility, practically non-existent in highly sensitive photoluminescence measurements, increases to a likelihood if simple optical absorption is the sole measurement technique. The determination of the onset of the band edge absorption is a source of large uncertainties, in addition to the fitting often involved in the determination of the band gap.

The electron effective masses from our calculations exhibit a slight anisotropy, as expected in a wurtzite structure. The effective mass is a measure of the curvature of the calculated bands. The agreement between calculated and measured effective masses indicates an accurate determination of the shape of the bands. We calculated the effective masses of the n-type carriers of ZnO, using the electronic structure from calculation II (the solid line in Fig. 1). Near the bottom of the lowest conduction band at the gamma point, we obtained 0.254, 0.260, and 0.264 m_0 in the Γ-A, Γ–K, and Γ-M directions, respectively, for the lattice constants in Figure 1. For the conduction band in Figure 2, the corresponding values are 0.257, 0.258, and 0.257 m_0 respectively. These values agree very well with the measured value of 0.24 m_0, within the experimental uncertainty [12] of 0.02 m_0, and with the experimental value of 0.275 m_o. [48] The above excellent agreement with experiment and the underestimates from previous LDA

calculations are graphically illustrated in Figure 1. Indeed, the drastic extra-lowering of the low lying conduction band (dotted lines in Fig. 1), in calculations employing basis sets larger than the optimal one, results in a significant decrease of the effective mass. In contrast, the lowest lying conduction band at Γ, as obtained with the optimal basis set (solid lines in Fig 1), leads to larger values of the electron effective mass.

IV. Conclusion

We have performed ab-initio, self-consistent calculations of the electronic energy bands, the density of states (DOS), and of the electron effective masses of wurtzite zinc oxide (w-ZnO). The implementation of the Bagayoko, Zhao, and Williams (BZW) procedure, within the linear combination of atomic orbitals, led to occupied and *unoccupied* energy bands respectively similar and *drastically different* from results of previous calculations. Our calculated band gap of 3.278 eV, at an experimental lattice constant, is only 5% smaller than the measured value of 3.44 eV. This work strongly indicates that the previous LDA band gaps that are 34% to 93% smaller than the experimental value suffer from the basis set and variational effect described above and possibly from other computational limitations; hence, their gross disagreement with experiment should no longer be ascribed to a failure of LDA. Our calculated electron effective masses are in excellent agreement with experiment, within experimental uncertainties.

Acknowledgments: This work was funded in part by the Department of the Navy, Office of Naval Research (ONR, Award Nos. N00014-05-1-0009 and N00014-04-1-0587), through the Timbuktu Academy, NASA (Award Nos. NCC 2-1344 and NAG 5-10253), the National Science Foundation (Award No. HRD 0000272), and by the Louisiana Board of Regents (Contract No. LEQSF(2002-03)-ENH-TR-57).

References

[1] H. Nowotny, F. Benesovsky, and R. Kieffer, Z. Metallk. 50, 258 (1959).
[2] D. G. Thomas, J. Phys. Chem. Solids 15, 86 (1960).
[3] Y. S. Park, C. W. Litton, T. C. Collins, and D. C. Reynolds, Phys. Rev. 143, 512 (1966).
[4] W. Y. Liang and A. D. Yoffe, Phys. Rev. Lett. 20, 59 (1968). Their samples of 0.1 μm thickness were films.
[5] K. Hümmer, Phys. Stat. Sol. (b) 56, 249 (1973).
[6] R. Matz and H. Lüth, Appl. Phys. 18, 123-130 (1979).
[7] D. C. Reynolds, D. C. Look, B. Jogai, C. W. Litton, G. Cantwell, and W. C. Harsch, Phys. Rev. B 60, 2340 (1999).
[8] V. Srikant and D. R. Clarke, J. Appl. Phys. 83, 5447 (1998).
[9] R. A. Powell, W. E. Spicer, and J. C. McMenamin, Phys. Rev. B 6, 3056 (1972).
[10] G. Zwicker and K. Jacobi, Solid State Communications 54, 701 (1985).
[11] R. T. Girard, O. Tjernberg, G. Chiaia. S. Söderholm, U. O. Karlsson, C. Wigren, H. Nylen, I. Lindau, Surface Science 373, 409-417 (1997).
[12] W. S. Baer, Phys. Rev. 154, 785 (1967).

[13] S. Desgreniers, Phys. Rev. B 58, 14102 (1998).
[14] S. A. Studenikin, N. Golego, and M. Cocivera, J. Appl. Phys. 83, 2104 (1998).
[15] P. L. Washington, H. C. Ong, J. Y. Dai, and R. P. H. Chang, Appl. Phys. Lett. 72, 3261 (1998).
[16] J. F. Muth, R. M Kolbas, A. K. Sharma, S. Oktyabrsky, and J. Narayan, J. Appl. Phys. 85,7884 (1999).
[17] Th. Pauporté and D. Lincot, Appl. Phys. Lett. 75, 3817 (1999).
[18] X. W. Sun and H. S. Kwok, J. Appl. Phys. 86, 408 (1999).
[19] M. Rebien, W. Henrion, M. Bär, and Ch. -H. Fischer, Appl. Phys. Lett. 80, 3518 (2002).
[20] B. S. Li, Y. C. Liu, Z. Z. Zhi, D. Z. Shen, Y. M. Lu, J. Y. Zhang, X. G. Kong, X. W. Fan, Thin Solid Films 414, 170-174 (2002).
[21] J. E. Jaffe, R. Pandey and A. B. Kunz, J. Phys. Chem. Solids 52, 755 (1991).
[22] J. E. Jaffe and A. C. Hess, Phys. Rev. B 48, 7903 (1993).
[23] S. Massidda, R. Resta, M. Posternak, and A. Baldereschi, Phys. Rev. B 52, 16977 (1995).
[24] H. Karzel, W. Potzel, M. Köfferlein, W. Schiessl, M. Steiner, U. Hiller, G. M. Kalvius, D. W. Mitchell, T. P. Das, P. Blaha, K. Schwarz, and M. P. Pasternak, Phys. Rev. B 53, 11425 (1996).
[25] J. R. Chelikowsky, Solid State Comm. 22, 351 (1977).
[26] U. Rössler, Phys. Rev. 184, 733 (1969).
[27] P. Schröer, P. Krüger, and J. Pollmann, Phys. Rev. B 47 6971 (1993).
[28] D. Vogel, P. Krüger, and J. Pollmann, Phys. Rev. B 52, 14316 (1995).
[29] Salehpour and S. Satpathy, unpublished, as cited by others.
[30] M. Usuda, N. Hamada, T. Kotani, and M. van Schilfgaarde, Phys. Rev. B 66, 125101 (2002).
[31] M. Oshikiri and F. Aryasetiawan, Journal of Physical Society of Japan 69, 2113 (2000).
[32] A. Svane and E. Antoncik, Phys. Rev. B, 33, 7462 (1986).
[33] W. R. L. Lambrecht, A. V. Rodina, S. Limpijumnong, B. Segall, and B. K. Meyer Phys. Rev. B 65, 075207 (2002).
[34] M. Oshikiri, F. Aryasetiawan, Y. Imanaka, and G. Kido, Phys. Rev. B 66, 125204 (2002).
[35] Y. -N. Xu and W. Y. Ching, Phys. Rev. B 48, 4335 (1993).
[36] D. Bagayoko, G. L. Zhao, J. D. Fan, and J. T. Wang, Journal of Physics: Condensed Matter, 10, 5645 (1998).
[37] G. L. Zhao, D. Bagayoko, and T. D. Williams, Physical Review B 60, 1563 (1999).
[38] G. L. Zhao and D. Bagayoko, New Journal of Physics, 2, 16.1-16.12 (2000), online 18 July 2000.
[39] G. L. Zhao, D. Bagayoko, and E. G. Wang, Accepted for publication in Phys. Rev. B 69, 1 (2004).
[40] P. Hohenberg and W. Koim, Phys. Rev. 136, B864 (1964).
[41] W. Kohn and L. J. Sham, Phys. Rev. 140, A1133 (1965).
[42] L. Hedin and S. Lundqvist, Solid State Physics 23, 1 (1969).
[43] D. M. Ceperley and B. J. Alder, Phys. Rev. Lett. 45, 566 (1980).
[44] S. H. Vosko, L. Wilk, and M. Nusair, Can. J. Phys. 58, 1200 (1980).

[45] P. J. Feibelman, J. A. Appelbaum, and D. R. Hamann, Phys. Rev. B 20, 1433 (1979).
[46] B. N. Harmon, W. Weber, and D. R. Hamann, Phys. Rev. B 25, 1109 (1982).

[47] R. W. G. Wyckoff, *Crystal Structures*, vol. 1, (John Wiley & Sons, New York, 1960), p.111.
[48] Landolt-Börnstein New Series III, vol. 22a, *Zahlenwerte und Funktionen aus Naturwissenschaften und Technik*, edited by O. Madelung and M. Schulz (Springer, New York, 1987).

Table 1. Calculated, fundamental band gaps (Eg, in eV) of w-ZnO, along with pertinent lattice constants in Angstroms, compared to experiment. Numbers in the last four columns, for a given row, are from the reference cited in that row.

	Computational Method	**a (Å)**	**c (Å)**	**u**	**Eg (eV)**
Local Density Approximation (LDA) Potentials	LCAO-BZW (Present work)	3.2501	5.2071	0.3817	3.20
		3.2496	**5.206**	**0.345**	**3.28**
		3.2530	5.2130	0.3817	3.21
		3.2700	5.1800	0.381	3.22
	Zn^{2+} Pseudopotential	3.25	5.21		2.13[a]
	Zn^{12+} Pseudopotential	3.25	5.21		0.23[a]
	Pseudopotential	3.23	5.18		0.23[b]
	APW				1.40[c]
	LAPW	3.253	5.2129	0.3817	0.77[d]
	FLAPW				0.93[e]
	LMTO	3.2427	5.1948	0.3826	1.15[f]
	LMTO	3.2496	5.2065	0.345	0.97[f]
	LMTO	3.253	5.2129	0.3825	0.78[d]
	LMTO (cubic, a=4.57 Å)				2.26[g]
	FP-LMTO			0.382	1.813[h]
LDA & Additional Exchange	Orthogonalized LCAO	3.249	5.207	0.345	0.88[i]
LDA+SIC	Pseudopotential	3.29	5.29		3.77[b]
X^{α} Potential	Pseudopotential	3.25	5.21		1.58[a]
GWA	LMTO	3.2427	5.1948	0.3826	4.28 and 4.06[a]
GWA	LMTO	3.2496	5.2065	0.345	3.45 and 3.63[a]
GWA	LMTO	3.253	5.2129	0.3825	2.44[d]
GWA	LAPW	3.253	5.2129	0.3817	2.44[d]
Model GWA	FLAPW				4.23[e]
Empirical Pseudopotential (EMP)					3.5[j]
Empirical KKR					3.30[k]
Experiment (Bulk, Low Temperatures)					**3.44**
Experiment (Bulk, Room Temperature)					**3.30**

[a]Reference 27 [b]Reference 28 [c]Reference 29
[d]Reference 30 [e]Reference 23 [f]Reference 31
[g]Reference 32 [h]Reference 33 [i]Reference 35
[j]Reference 25 [k]Reference 26

Figure 1. Electronic band structures of wurtzite zinc oxide (w-ZnO) from Calculations II and III of the BZW method. The solid lines show the results of calculation II and the dashed lines represent the bands from calculation III. *Calculation II gives the final electronic structure of ZnO with the optimal basis set.* The Fermi levels from the two calculations are superimposed. The lattice constants are $a = 3.2501$ Angstroms (Å), $c = 5.2071$ Å, and $u = 0.3817$. The band gap is 3.2 electron volts (eV).

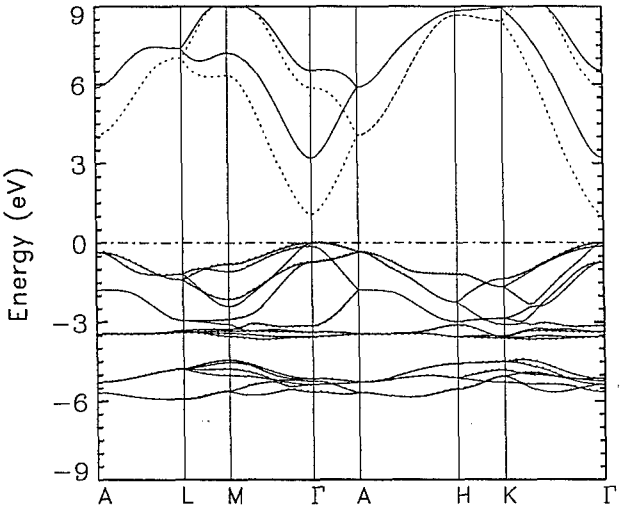

Figure 2. Calculated band structure of wurtzite zinc oxide (w-ZnO), as obtained with BZW method, for experimental lattice constants of $a = 3.2496$ Å, $c = 5.206$ Å, and $u = 0.345$. The band gap is 3.278 eV.

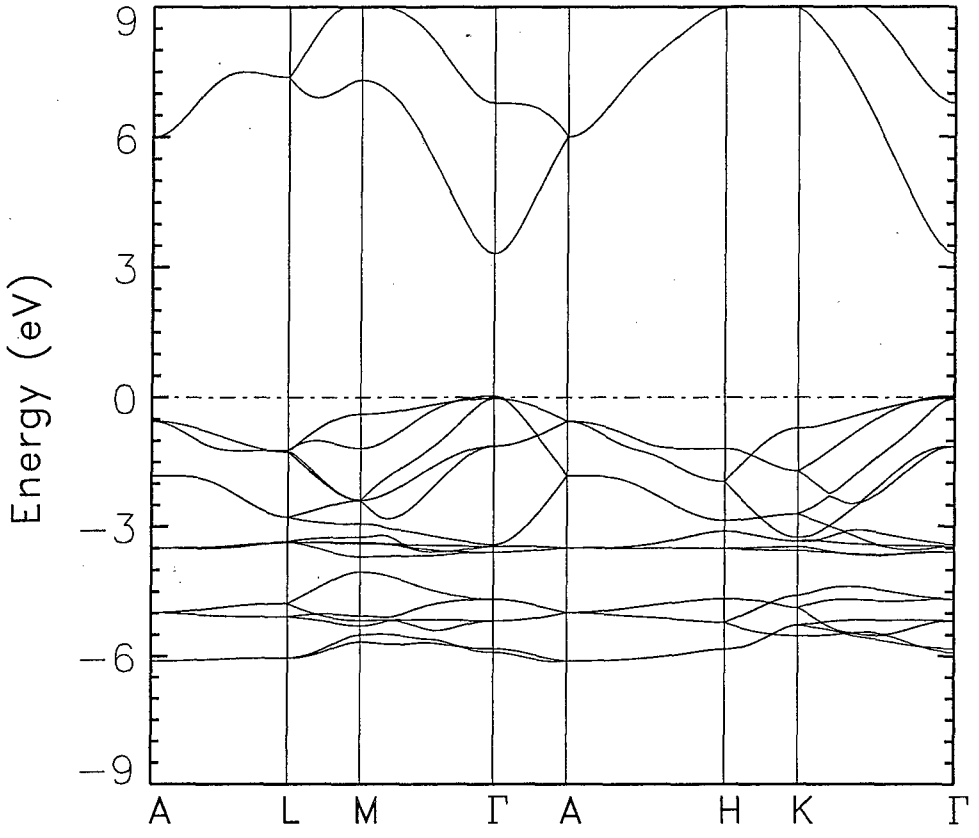

Figure 3. Calculated total density of state (DOS) for w-ZnO, as derived from the bands shown in Fig. 2. The inset indicates that experimental apparatus or techniques that are not very sensitive could find band gaps much larger than the theoretical minimum of 3.278 eV.

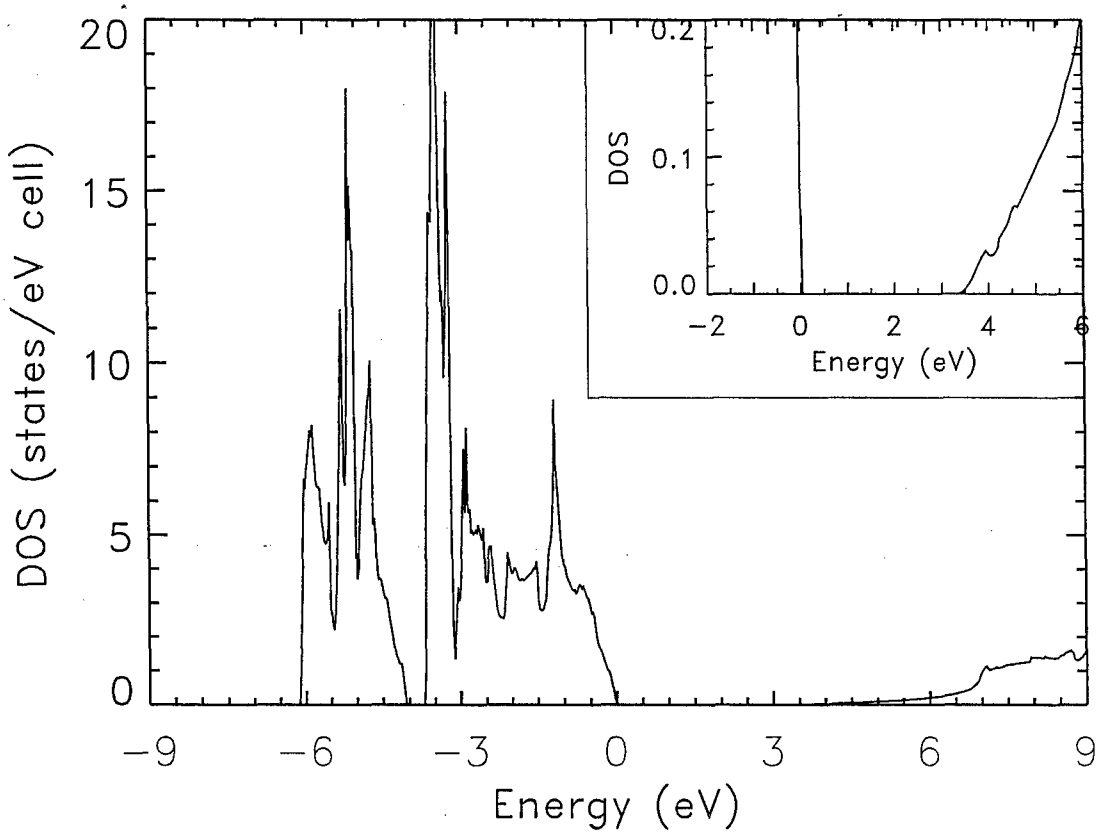

Figure 4. Calculated partial density of states (pDOS) for w-ZnO at the experimental lattice constants of $a = 3.2496$ Å, $c = 5.206$ Å, and $u = 0.345$. The graph illustrates the influence of the zinc d and the oxygen p in the upper valence bands. Zinc s dominates in the lowest conduction band.

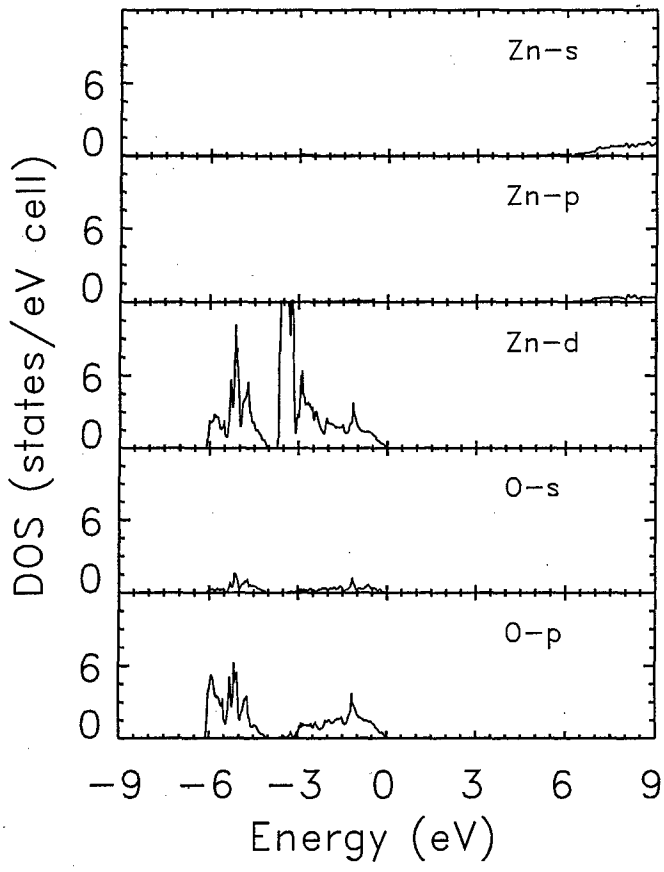

Reprinted from

JOURNAL OF APPLIED PHYSICS

Vol. 96, No. 8, 15 October 2004

Predictions of electronic, structural, and elastic properties of cubic InN

D. Bagayoko, L. Franklin, and G. L. Zhao
Department of Physics, Southern University and A&M College, Baton Rouge, Louisiana 70813

pp. 4297-4301

AMERICAN INSTITUTE OF PHYSICS

Predictions of electronic, structural, and elastic properties of cubic InN

D. Bagayoko, L. Franklin, and G. L. Zhao
Department of Physics, Southern University and A&M College, Baton Rouge, Louisiana 70813

(Received 25 May 2004; accepted 16 July 2004)

We present theoretical predictions of electronic, structural, and elastic properties of cubic indium nitride in the zine-blende structure (*c*-InN). Our *ab initio*, self-consistent calculations employed a local density approximation potential and the Bagayoko, Zhao, and Williams implementation of the linear combination of atomic orbitals. The theoretical equilibrium lattice constant is 5.017 Å, the band gap is 0.65 eV, and the bulk modulus is 145 GPa. The band gap is 0.74 eV at an experimental lattice constant of 4.98 Å. © *2004 American Institute of Physics*. [DOI: 10.1063/1.1790064]

I. INTRODUCTION AND MOTIVATIONS

Several review papers[1–4] have discussed the properties and applications of wurtzite and zinc-blende indium nitride (*c*-InN). In particular, the value of the band gap of wurtzite InN (*w*-InN) has recently attracted much interest[3–5] due to seemingly conflicting findings from experimental investigations. The current and potential applications of InN based semiconductor devices certainly warrant a rapid resolution of the unsettled issues relative to these important materials.[1–5] Indeed, light emitting diodes (LEDs), laser diodes (LDs), and photodiodes (PDs), over a wide range of energy, from ultraviolet to infrared wavelengths, are some of these applications of InN based semiconductors. The direct band gaps of high quality wurtzite InN films are reported[3–5] to be from 0.65 to 1 eV, depending on carrier concentration and other sample characteristics. The band gap of cubic InN (*c*-InN) is expected to be in this range or slightly below it. Hence, InN films could be critical for the fabrication of high speed LDs and PDs for optical communication systems.[3] Unlike *w*-InN, the most stable phase of InN in ordinary conditions, much remains to the known about *c*-InN. This situation is partly due to the serious difficulties associated with the growth of *c*-InN.[3,4]

These difficulties are apparent in the work of Yamamoto *et al.*[6] who grew *c*-InN on GaAs and α-Al_2O_3 substrates. They reported the appearance of *w*-InN when the film thickness was over 0.05 μm, and at thicknesses over 0.2 μm, the *c*-InN films grown on GaAs were completely covered by hexagonal indium nitride. The films grown on sapphire contained columnar, fibrous structures. Unlike Yamamoto *et al.*[6] who utilized metalorganic vapor-phase epitaxy (MOVPE) Tabata *et al.*,[7] Chandrasekhar *et al.*,[8] and Cimalla *et al.*[9] employed molecular beam epitaxy (MBE) to grow *c*-InN films. These authors reported values of the lattice constant of *c*-InN of 4.97±0.01, 4.980, and 4.986 Å, respectively. We are unaware of reports of experimental investigations of the electronic and elastic properties of *c*-InN. Hence, an aim of this work is to predict electronic and related properties of *c*-InN, including the band gap.

The need for this work is partly underscored by the disagreement between previous theoretical findings.[10–22] Previous local density approximation (LDA) calculations that employed the pseudopotential (PP) method produced negative band gaps ranging[10,11,13–15,19] from −0.18 to −0.40 eV. Other LDA calculations,[11,12,16,19] using variations of the linearized augmented plane wave (LAPW),[11,12] linear muffin-tin orbital (LMTO),[16] and the atomic sphere approximation (ASA) (Ref. 19) obtained *c*-InN band gaps of 0.08–0.48 eV. The generalized gradient approximation (GGA),[11,13] within the pseudopotential approach, led to a gap value[13] of −0.55 eV. Self-interaction corrections to LDA, quasiparticle (QP) approaches, and exact exchange calculations reported *c*-InN band gaps of 0.43–1.40 eV as shown in Table I below. The very recent empirical pseudopotential result of Fritsch *et al.*[22] is 0.592 eV for the band gap of *c*-InN. Our focus here is mainly on the LDA results that are very small or negative for the band gap of *c*-InN. This situation constitutes another motivation for this work, besides the lack of experimental data on the electronic and related properties of *c*-InN. Our LDA calculations recently resolved the controversy that was surrounding the band gap of wurtzite InN.[23] In particular, our LDA calculations, within the Bagayoko, Zhao, and Williams (BZW) implementation of the linear combination of atomic orbitals (LCAO) method, obtained a *w*-InN band gap of 0.88 eV, in very good agreement with measurements from a recent series of experimental investigations.[23]

Further, utilizing features of the calculated density of states (DOS), we showed[23] the possibility of obtaining a gap as large as 2 eV if optical absorption is the only measurement technique utilized. Difficulties in precisely determining the band edge, analysis techniques, and related uncertainties explain this assertion. Our work on *w*-InN added to a series of articles according to which it is no longer correct to state that local density approximation woefully underestimates the band gaps of semiconductors. Hence, and in the light of the mostly negative values of the band gap of *c*-InN, there exists a compelling rationale for an implementation of the LDA that does not suffer from an effect[24–26] believed to be mostly responsible of the dismal underestimation of band gaps. Incidentally, the band gap problem was actually a symptom of a more general and unrecognized problem stemming from unoccupied levels or bands that are affected by the effect referenced above and recalled below.

 © 2004 American Institute of Physics

TABLE I. Experimental and theoretical lattice constants (a, in angstroms) for *c*-InN, along with the calculated values of the bulk modulus gigapascal and of the fundamental band gap (eV). Results in the last three columns, for a given row, are from the reference cited in that row.

	Computational Method	a(Å)	B(GPa)	Eg(eV)
	LCAO-BZW (Present work)	5.017	145	+0.65
		4.98		+0.74
	Pseudopotential Method (PP)	4.95	145	−0.36[a]
		5.004	140	−0.40[b]
		4.95	145[c]	
		4.97[d]		
		4.932	140	−0.35[e]
Local Density Approximation (LDA) Potentials		4.788	155[f]	
				−0.18[g]
	LAPW	4.94	145[c]	
	Full potential LAPW	5.03	138	−0.11[h]
				−0.48[h]
	Full Potential LMTO	4.92	139[j]	−0.4[i]
	Atomic sphere approximation (ASA)			−0.1[l]
				+0.02 and +0.08[k]
Generalized gradient approximation (GGA)	PP	5.06	120[c]	
		5.109	118	−0.55[b]
LDA plus self-interaction correction (SIC)		5.05[d]		+0.43[a]
QP Calculation	PP			+0.52[a]
QP+SIC	PP			+1.31[a]
DFT Exact Exchange				+1.4[g]
DFT, SX	ASA			+1.3[i]
Estimate of the bulk modulus of zinc-blende indium nitride (*c*-InN) using elastic properties of wurtzite InN			137[l]	
Empirical Pseudopotential Calculations (EMP)				+0.592[m]
Experimental: Measured lattice constants		4.97±0.01[n]		
		4.98[o]		
		4.986[p]		

[a]Reference 10.
[b]Reference 13.
[c]Reference 11.
[d]Reference 15.
[e]Reference 18.
[f]Reference 21.
[g]Reference 14.
[h]Reference 12.
[i]Reference 16.
[j]Reference 17.
[k]Reference 19.
[l]Reference 20.
[m]Reference 22.
[n]Reference 7.
[o]Reference 8.
[p]Reference 9.

II. METHOD AND COMPUTATIONAL DETAILS

We performed zero temperature, nonrelativistic calculations of the electronic and related properties of *c*-InN. Our *ab inito*, self-consistent calculations employed the local density approximation potential of Ceperley and Alder[27] as parametrized by Perdew and Zunger.[28] As stated above, we used the LCAO. The feature distinguishing our computational method from the previous investigations noted above consists of our implementation of the BZW procedure. In so doing, we started the calculations for *c*-InN with a minimal basis set. We subsequently performed several other self-consistent calculations with larger and larger basis sets. The basis set for any of these calculations was obtained by augmenting the one for the previous calculation with the orbital describing the next excited level of the atomic or ionic species present in the system. The occupied bands of a given calculation are compared to those of the previous. These comparisons, particularly for the first two calculations, often show differences (in numerical values, branching, or curvature). This process continues until the occupied energies from a calculation are equal, within computational uncertainties, to their corresponding ones from the calculation that follows it. Then, the output of the former calculation provides the physical description of the material under study and the related basis set is dubbed the optimal basis set. According to the Rayleigh theorem,[26] some of the *unoccupied bands* from the latter may be lower than their counterpart from the former.[24–26,29,30]

The above additional lowering is the *basis set* and *variational* effect inherently associated with variational calculations of the Rayleigh-Ritz type. In the iterative process, the use of the wave functions for the occupied states *only* in the construction of the charge density, and hence the potential and the Hamiltonian, ensures the exhaustion of the accounting for the physical interactions when the occupied energies converge vis-a-vis the size of the basis set. As fully explained elsewhere,[24–26,29] however, some unoccupied energies will continue to be lowered as the basis set is increased beyond the optimal one. The sizes of the minimal and optimal basis sets vary vastly with the type of functions in the

TABLE II. Eigenvalues (eV), along high symmetry points, for zinc-blende indium nitride (c-InN) as obtained from LDA-BZW calculations for a =5.017 Å, the theoretical equilibrium value. The Fermi energy of −0.216 87 eV is set to zero in the table.

L	Γ	X	K
−15.5192	−14.8427	−15.6493	−15.5949
−14.7559	−14.8427	−14.7301	−14.7034
−14.7559	−14.8427	−14.5254	−14.5837
−14.4740	−14.5336	−14.5254	−14.5739
−14.4740	−14.5336	−14.4463	−14.4865
−11.7624	−14.1793	−11.3085	−11.2078
−5.5713	0.0000	−4.7495	−4.5900
−0.8335	0.0000	−2.2093	−3.3631
−0.8335	0.0000	−2.2093	−1.7848
4.0316	0.6536	4.1816	5.6110
8.4339	9.7615	6.8978	7.1493
10.6892	9.7615	11.8922	10.5553
10.6892	9.7615	11.8922	11.6130

atomic orbitals (i.e., exponential, Gaussian, plane wave functions) and with other features of the calculations (i.e., pseudopotential, LAPW, etc). As described above, the BZW method is applicable in most computations that utilize the LCAO formalism. The LCAO program package we employed in this work was developed many years[31–33] before the introduction of the BZW method in 1998. We provide below computational details germane to a replication of our calculations.

Zinc-blende InN is a member of the III-V family. The atomic wave functions of the ionic states of In^{1+} and N^{1-} were obtained from self-consistent *ab initio* calculations. The radial parts of the atomic wave functions were expanded in terms of Gaussian functions. A set of even-tempered Gaussian exponents was employed for In with a minimum of 0.1400 and a maximum of 0.2300×10^{6}, with 16 Gaussian functions for the s and p states and 14 for the d states of In^{1+}. The two largest exponents were not included in the description of the d state. Similarly, a set of even-tempered Gaussian exponents was utilized to describe N^{1-}, with a minimum of 0.1242 and a maximum of 0.1365×10^{5}. Both the s and p functions were expanded in terms of 13 Gaussian orbitals. The minimal basis set comprised atomic orbitals representing In^{1+} ($1s2s2p3s3p3d4s4p4d5s5p$) and N^{1-} (1s2s2p). A mesh of $28k$ points in the irreducible Brillouin zone, with proper weights, was used in the self-consistent iterations. The computational error for the valence charge was about −0.001 449 79 for 36 electrons. The self-consistent potentials converged to a difference around 10^{-5} after about 60 iterations.

TABLE III. Eigenvalues (eV), along high symmetry points, for zinc-blende indium nitride (c-InN), as obtained from LDA-BZW calculation for a =4.98 Å. The Fermi energy −0.216 58 eV is set to zero the table.

L	Γ	X	K
−15.5977	−14.8586	−15.7269	−15.6720
−14.7642	−14.8586	−14.7370	−14.7084
−14.7642	−14.8586	−14.5160	−14.5781
−14.4583	−14.5212	−14.5160	−14.5685
−14.4583	−14.5212	−14.4279	−14.4714
−11.7856	−14.3473	−11.3252	−11.2093
−5.7063	0.0000	−4.8350	−4.6807
−0.8675	0.0000	−2.2907	−3.4730
−0.8675	0.0000	−2.2907	−1.8515
4.1748	0.7383	4.2140	5.6870
8.5382	9.9148	7.1020	7.3237
10.8738	9.9148	12.1018	10.7467
10.8738	9.9148	12.1018	11.8177

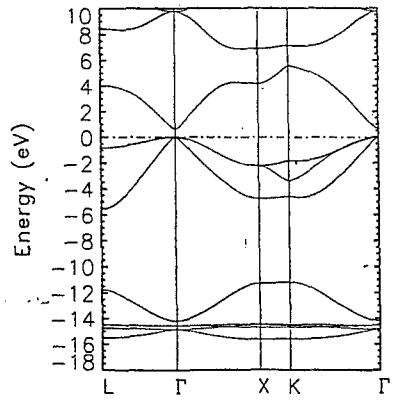

FIG. 1. Calculated LDA-BZW band structure of zinc-blende Indium Nitride (c-InN) at the theoretical equilibrium lattice constant of 5.017 Å, as obtained with BZW optimal basis set. The Fermi level (−0.216 87 eV) is set to zero in the figure.

III. RESULTS AND DISCUSSIONS

Table I shows our calculated, theoretical equilibrium band gap of 0.65 eV, at a lattice constant of 5.017 Å, and the value of 0.74 eV at an experimental lattice constant of 4.98 Å. Tables II and III contain the calculated energies, at some high symmetry points in the Brillouin zone, for the two lattice constants given above. Figures 1–3 exhibit the energy bands, for the theoretical equilibrium lattice constant (5.017 Å), and the related total (DOS) and partial (pDOS) densities of states. The curve of the total energy versus the lattice constant is shown in Fig. 4.

The lack of experimental data, except for the lattice constant, precludes an extensive discussion of these results. Our predicted equilibrium lattice constant is within 0.6% from

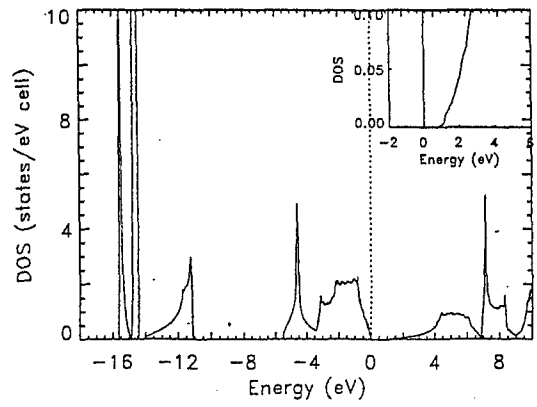

FIG. 2. Total DOS for zinc-blende indium nitride (c-InN) as obtained with the bands shown in Fig. 1. The inset illustrates our definition of a "practical band gap."

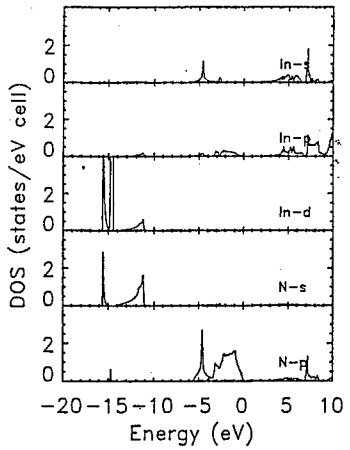

FIG. 3. pDOS for zinc-blende indium nitride (c-InN) as obtained with the bands shown in Fig. 1. The dominance of nitrogen p at the top of the valence band is obvious in this graph.

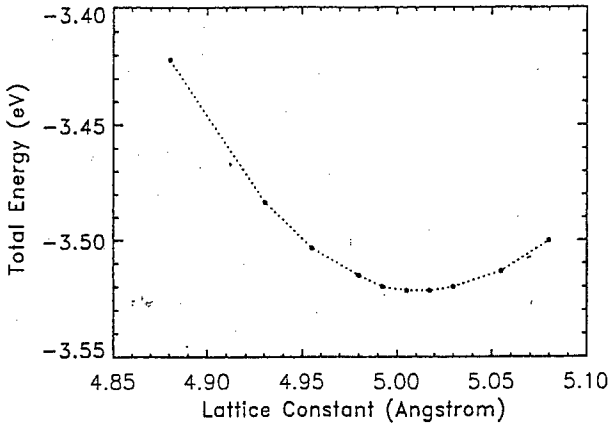

FIG. 4. Total energy of (c-InN) vs the lattice constant. The total energy at the equilibrium lattice constant of 5.017 Å is 1949.4215 eV.

the latest experimental one of 4.986 Å. Our calculated bulk modulus of 145 GPa is close to the results from some other LDA calculations[10,11] and disagrees with findings around 120 GPa from GGA calculation[11,13] as shown in Table I. The tables for the calculated energies are expected to provide useful comparisons for future experimental investigations. Our calculated LDA-BZW band structure is drastically different from the findings of most of the previous calculations—as far as the unoccupied bands are concerned. The large differences between our calculated band gaps and previous LDA results in Table I are a direct consequence of the differences between the respective *unoccupied* bands.

The empirical pseudopotential (EMP) result[22] of 0.592 eV is relatively close to our findings of 0.65 and 0.74 eV. We cannot draw much fundamental significance from this fact, however, given that this EMP result was obtained using model potential parameters whose derivation entailed fitting to data that included a band gap of 0.59 eV. For the purposes of application, however, this closeness portends much importance. Indeed, we expect potential parameters derived from fitting to our data to lend themselves to credible and practical descriptions of electronic, optical, elastic, and structural properties of materials. This assertion is partly supported by the versatility and relative ease of empirical pseudopotential calculations.

As in the case of w-InN,[23] our results do not show any indication of an overestimation of the p-d repulsion by LDA potentials. This overestimation was believed[10] to be the source of the very small or negative band gaps by pushing the top of the valence band, dominated by p states, to higher energies. According to our findings, it is rather the extra lowering of the bottom of the conduction band that produces LDA band gaps that are negative or very small[23,25] if LCAO type computations do not utilize the BZW approach to avoid it while ensuring the adequacy (or convergence) of the basis set for the description of occupied states. In fact, the basic derivation of the ground state theory that is the original density functional theory[34,35] implicitly suggests such an approach, notwithstanding the need to account for the redistribution of electrons in molecular to solid environments with judicious polarization and diffuse orbitals.[36]

As per their definition, effective masses provide a measure of the quality (i.e., curvature) of band structures. Our LDA-BZW calculations found electron effective masses, at the bottom of the conduction band, of $0.065m_0$, $0.066m_0$, and $0.066m_0$ in the Γ-L, Γ-X, and Γ-K directions, respectively, for the equilibrium lattice constant. For a lattice constant of 4.98 Å, the corresponding effective masses for the electrons are $0.076m_0$, $0.073m_0$, and $0.073m_0$ in the Γ-L, Γ-X, and Γ-K directions, respectively. Our calculated, equilibrium, electron effective masses are very close to the $0.066m_0$ from the EMP calculations of Fritsch, Schmidt, and Grundmann.[22] This agreement supports our comment above relative to the potential use of EMP calculations when the potential parameters are derived in part by fitting to LDA-BZW results.

IV. CONCLUSION

In lieu of a conclusion, we contend that our *ab initio*, self-consistent LDA-BZW calculations have predicted electronic, structural, and elastic properties of cubic InN (c-InN) in the zinc-blende structure. It is hoped that experimental investigations will follow in the near future. It emerges from this work that theoretical efforts should be directed to the determination of actual limitations of LDA and of other approaches as opposed to echoing the chorus now known to be untenable, as per the physical interactions, and that ascribes to LDA a woeful underestimation of band gaps that is, as per the Rayleigh theorem, straightforwardly a consequence of a basis set and variational effect.

ACKNOWLEDGMENTS

This work was funded in part by the Department of the Navy, Office of Naval Research (ONR, Grant No. N00014-98-1-0748), NASA (Award Nos. NCC 2-1344 and NAG 5-10253), and by the National Science Foundation (Grant No. HRD 0000272). The authors are indebted to Dr. J. Wu for bringing the band gap problem for cubic InN to their attention.

[1]J. W. Orton and C. T. Foxon, Rep. Prog. Phys. 1 (1998).
[2]O. Ambacher, J. Phys. D 31, 2653 (1998).
[3]A. G. Bhuiyan, A. Hashimoto, and A. Yamamoto, J. Appl. Phys. 94, 2779 (2003).

[4]I. Vurgaftman and J. R. Meyer, J. Appl. Phys. 94, 3675 (2003).
[5]J. Wu *et al.*, Appl. Phys. Lett. 80, 3967 (2002).
[6]A. Yamamoto, Y. Yamauchi, M. Ohkubo, and A. Hashimoto, J. Cryst. Growth 174, 641 (1997).
[7]A. Tabata *et al.*, Appl. Phys. Lett. 74, 362 (1999).
[8]D. Chandrasekhar, David J. Smith, S. Strite, M. E. Lin, and H. Morkoc, J. Cryst. Growth 152, 135 (1995).
[9]V. Cimalla *et al.*, Appl. Phys. Lett. 83, 3468 (2003).
[10]F. Bechstedt and J. Furthmüller, J. Cryst. Growth 246, 315 (2002).
[11]M. Fuchs, J. L. F. Da Silva, C. Stampfi, J. Neugebauer, and M. Scheffler, Phys. Rev. B 65, 245212 (2002).
[12]L. E. Ramos, L. K. Teles, L. M. R. Scolfaro, J. L. P. Castineira, A. L. Rosa, and J. R. Leite, Phys: Rev. B 63, 165210 (2001).
[13]C. Stampfl and C. G. Van de. Walle, Phys. Rev. B 59, 5521 (1998).
[14]M. Stäedele, J. A. Majewski, P. Vogl, and A. Görling, Phys. Rev. Lett. 79, 2089 (1997).
[15]D. Vogel, P. Krüger, and J. Pollmann, Phys. Rev. B 55, 12836 (1997).
[16]M. van Schilfgaarde, A. Sher, and A. B. Chen, J. Cryst. Growth 178, 8 (1997).
[17]K. Kim, Walter R. L. Lambrecht, and B. Segall, Phys. Rev. B 53, 16310 (1996).
[18]A. F. Wright and J. S. Nelson, Phys. Rev. B 51, 7866 (1995).
[19]N. E. Christensen and I. Gorczyca, Phys. Rev. B 50, 4397 (1994).
[20]M. E. Sherwin and T. J. Drummond, J. Appl. Phys. 69, 8423 (1991).
[21]P. E. Van Camp, V. E. Van Doren, and J. T. Devreese, Phys. Rev. B 41, 1598 (1990).
[22]D. Fritsch, H. Schmidt, and M. Grundmann, Phys. Rev. B 69, 165204 (2004).
[23]D. Bagayoko and L. Franklin, J. Appl. Phys. (submitted).
[24]D. Bagayoko, G. L. Zhao, J. D. Fan, and J. T. Wang, J. Phys.: Condens. Matter 10, 5645 (1998).
[25]G. L. Zhao, D. Bagayoko, and T. D. Williams, Phys. Rev. B 60, 1563 (1999).
[26]D. Bagayoko, Int. J. Quantum Chem. 17, 527 (1983).
[27]D. M. Ceperley and B. J. Alder, Phys. Rev. Lett. 45, 566 (1980).
[28]J. P. Perdew and A. Zunger, Phys. Rev. B 23, 5048 (1981).
[29]D. Bagayoko, G. L. Zhao, and S. Hasan, in *A Mathematical Solution of the Band Gap Problem*, in Contemporary Problems In Mathematical Physics, edited by Jan Govaerts, M. Norbert Hounkonnou, and Alfred Z. Msezane (World Scientific, London, 2002), 222–232.
[30]G. L. Zhao, D. Bagayoko, and E. G. Wang, Phys. Rev. B 69, 1 (2004).
[31]P. J. Feibelman, J. A. Appelbaum, and D. R. Hamann, Phys. Rev. B 20, 1433 (1979).
[32]B. N. Harmon, W. Weber, and D. R. Hamann, Phys. Rev. B 25, 1109 (1982).
[33]G. L. Zhao, T. C. Leung, B. N. Harmon, M. Keil, M. Muller, and W. Weber, Phys. Rev. B 40, 7999 (1989).
[34]P. Hohenberg and W. Kohn, Phys. Rev. 136, B864 (1964).
[35]W. Kohn and L. J. Sham, Phys. Rev. 140, A1133 (1965).
[36]D. Bagayoko, Pui-Man, N. Brener, and J. Callaway, Phys. Rev. B 54, 12184 (1996).

Reprinted from

JOURNAL OF APPLIED PHYSICS

Vol. 97, No. 12, 15 June 2005

Density-functional theory band gap of wurtzite InN

D Bagayoko and Lashounda Franklin
Department of Physics, Southern University and A&M College, Baton Rouge, Louisiana 70813

pp 123708 1-5

AMERICAN INSTITUTE OF PHYSICS

Density-functional theory band gap of wurtzite InN

D. Bagayoko[a] and Lashounda Franklin
Department of Physics, Southern University and A&M College, Baton Rouge, Louisiana 70813

(Received 7 September 2004; accepted 26 April 2005; published online 20 June 2005)

We report the calculated band gap of wurtzite indium nitride. Our *ab initio* computations employed a local-density approximation (LDA) potential and the linear combination of Gaussian orbital formalism. The implementation of the *ab initio* Bagayoko, Zhao, and Williams method [Phys. Rev. B 60, 1563 (1999)] led to a LDA band gap of 0.88 eV, in excellent agreement with recent experiments. We also present calculated density of states (DOS) and the electron effective mass at the bottom of the conduction band. Our DOS curves indicate that an experiment could find values of the band gap up to 2 eV, depending on the sensitivity of the apparatus, the interpretation of resulting data, and associated uncertainties. © *2005 American Institute of Physics.*
[DOI: 10.1063/1.1939069]

BACKGROUND AND MOTIVATIONS

The 1998 review articles of Orton and Foxon[1] and of Ambacher[2] extensively described the technological importance and potential of group III-nitrides, including InN. The ternary alloy $In_{1-X}Ga_XN$ offers a wide range of band gaps that depend on X. Until recently, the lower limit of this range was believed[1,2] to be about 1.8–2.0 eV. This limit was the previously measured band gaps of wurtzite InN as obtained from the absorption studies of mostly polycrystalline films grown by dc discharge,[3] various sputtering techniques,[4–8] or metal-organic vapor-phase epitaxy (MOVPE).[9] The above measured band gaps of wurtzite InN, i.e., 1.8–2.0 eV, are in disagreement with findings of recent experiments discussed below.

The 2000 study of the band bowing of InAlN by Yamaguchi *et al.*[10] strongly indicated that the band gap (E_g) of wurtzite InN should be less than 1.9 eV. Subsequent measurements of the band gap of InN films, mostly grown by molecular-beam epitaxy (MBE), agreed on a range of 0.7–1.0 eV. The high quality of the samples in these experiments was partly utilized to explain the large difference between the early[3–9] and latter[10–17] groups of experiments. Inishima *et al.*[11] found the value of E_g to be 0.89 and 1.46 eV for InN films at respective electron concentrations of 5×10^{19} and 2×10^{20} cm^{-3}. The multipronged study by Wu *et al.*[12] determined the band gap of *w*-InN by optical absorption, photoluminescence, and photomodulated reflectance techniques. The room-temperature band gap was found to be between 0.7 and 0.8 eV for their high-quality films that were grown by molecular-beam epitaxy. These authors further established that no noticeable feature could be found in the absorption and photomodulated reflectance spectra to indicate a band gap between 1.9 and 2.0 eV. The band-gap bowing of InGaN also pointed to a value[13] of E_g near 0.8 eV for wurtzite InN. Even though Matsuoka *et al.*[15] studied samples of wurtzite InN (*w*-InN) grown by metal-organic vapor-phase epitaxy, one of the growth methods of the early group of experiments, they found that E_g for their *w*-InN samples was between 0.7 and 1.0 eV. The 2004 work of Arnaudov *et al.*[17] on InN films grown by MBE or MOVPE gives a value of 0.692±0.002 eV for the low-temperature (2 K) band gap of high-quality samples with relatively low electron concentrations (i.e., 7.7×10^{17}–6×10^{18} cm^{-3}). These authors employed near-band-edge photoluminescence. The above agreement of recent experiments on E_g values between 0.7 and 1.0 eV, depending on temperature, pressure, and carrier concentration, is in stark contrast with the large range of the following theoretical findings.

Early empirical pseudopotential model calculations[18,19] (EPM) basically reproduced the gap of 2.0 eV reported by the above first group of experiments. The fitting involved in the method practically permits the reproduction of any selected feature of the electronic structure. The 2003 EPM work of Fritsch *et al.*[20] not only reproduced an earlier experimental band gap of 2.11 eV, but also reported values of 2.58 and 2.59 eV, for wurtzite InN, from their anisotropic and isotropic pseudopotential calculations.

Local-density approximation (LDA) results for the band gap of wurtzite InN, including those of authors who also performed quasiparticle[21,22] and other calculations, range[21–27] from −0.4 to 0.43 eV. The pseudopotential[22,24–26] (PP) and the full potential linearized augmented plane-wave[21,23] (FLAPW) calculations mostly reported negative values of the band gap, from −0.4 to −0.19 eV. The full potential linear muffin-tin orbital[23] (FP-LMTO) and atomic sphere approximation (ASA) approaches led to values between 0.2 and 0.43 eV.

A pseudopotential calculation within the generalized gradient approximation[25] (GGA) produced a band gap of −0.37 eV. Several authors reported the band gap of wurtzite InN as obtained by quasiparticle[22,25] (QP) or other computations that employed various schemes that either go beyond the local-density approximation[22,24,28] or alter LDA potentials.[21,27,29] In particular, the pseudofunction[28] approach, self-interaction correction (SIC),[22] and self-interaction with relaxation corrections (SIRC),[24] respectively, led to band gaps of 1.3, 0.58, and 1.6 eV. The GW method led to results[22,27] of 0.74 and 0.5 eV. The GW-SI produced a

[a]Electronic mail: bagayoko@phys.subr.edu

 © 2005 American Institute of Physics

gap of 1.5 eV. The linear combination of Gaussian orbital (LCGO) calculations of Xu and Ching[29] employed a LDA potential plus additional exchange effects obtained with Wigner interpolation formula. They reported a band gap of 1.02 eV. The LDA+C work of Wei *et al.*[27] augmented the LDA potential with atom-dependent corrections and obtained a band gap of 0.85 eV with an uncertainty of 0.1 eV.

Clearly, the above state of theoretical calculations is amply sufficient to motivate the present work. A recent experimental development[30] exacerbated the urgency of our theoretical investigations. Indeed, the concordant findings of the second group of experiments, described above, have just been questioned by Shubina *et al.*[30] in 2004. These authors showed the possibility of explaining the spectra of this second group of experiments not in terms of near-band-edge absorption or emission, but rather as manifestations of surface/gap states or Mie resonances due to In precipitates in InN. They noted the poor thermal stability of InN and the low In vapor pressure to support their position. Specifically, for high-quality InN films grown at $T>500$ °C by MBE or MOVPE, they utilized x-ray diffraction to observe tetragonal In precipitates in hexagonal InN. Their very low-temperature (0.35 K) measurements by thermally detected optical absorption (TDOA) indicate the possibility of having a band gap around 1.4 eV. The authors refrained from making a definitive statement as to the location of the fundamental band gap, despite their observations, due to the difficulties in separating the intraband absorption in InN from Mie resonances.

METHOD AND COMPUTATIONAL DETAILS

Our calculations employed the Ceperley and Alder[31] local-density-functional potential as parametrized by Perdew and Zunger[32] in an *ab initio* LCGO formalism. We also employed the GGA potential of Perdew and co-workers[33] which goes beyond LDA. The calculations are nonrelativistic and for zero temperature. A key distinction between this work and previous calculations resides in our utilization of the *ab initio* Bagayoko, Zhao, and Williams[34,35] (BZW) method in carrying out the self-consistent computations. Introduced[34] in 1998 and extensively employed[35–38] thereafter, this method rigorously avoids a basis set and variational effect inherently associated with all variational calculations that utilize both the linear combination of atomic orbital (LCAO) and a charge density obtained only with the wave functions of the occupied states. The effect, a consequence of the Rayleigh theorem, consists of a lowering of unoccupied energy levels or bands, which is not ascribable to a physical interaction, after the total convergence of the charge density, the potential, and of the occupied energy levels with respect to the size of the basis set.[34,35]

BZW self-consistent calculations begin with the minimum basis set, i.e., one that is just large enough to include all the orbitals for the occupied levels in the atomic species that are present in the system under study. This initial basis set, in our case, is derived from calculations for the atomic or ionic species present in the finite or infinite system under investigation. Completely self-consistent calculations with this basis set are generally not expected to describe the system correctly. Indeed, they generally do not account for electron redistribution in the system as opposed to that in neutral atoms or ionic species. A second self-consistent calculation is performed with a basis set that includes the minimum basis set as augmented with the orbital representing the lowest excited levels in the atomic (or ionic species). The occupied energy levels or bands of calculations I and II are compared. One generally finds differences between these energies from the two calculations. For solids, these differences are in numerical values and the branching and curvatures of the bands. A third calculation is performed by augmenting the basis set of calculation II as described above. If a comparison of the self-consistent, occupied energies of calculations II and III do not show a complete agreement, within applicable errors, the process of augmenting the basis set is continued. Eventually, calculations N and $(N+1)$ will have the same occupied energies. Further, the charge density and the potential, from these two calculations, are, respectively, the same.[34,35] Upon the convergence of the variational calculations with respect to the size of the basis, the results for calculation N are selected as the physical ones. One generally finds, indeed, that calculation $(N+1)$ produced some unoccupied energies that are lower than the corresponding ones in calculation N. These differences that vary vastly with the value of $\vec{k}$ in reciprocal space are manifestations of the aforementioned basis set and variational effect.[34–38] The basis set for calculation N is called the optimal basis set.

Other ordinary features of our calculations are thoroughly described in the literature in seminal papers that reported on the development[39–41] of the program package and its recent utilization.[34,35,38] We provide below computational details germane to a replication of our *ab initio* work. The experimental,[3] low-temperature wurtzite lattice parameters utilized in our work are $a=3.544$ Å, $c=5.718$ Å, and $u=0.3790$. Preliminary calculations for the neutral In and N atoms and the solid w-InN indicated that the self-consistent system is approximately $In^{0.8+}N^{0.8-}$. Consequently, we performed self-consistent calculations for In^{1+} and N^{1-} to obtain the input, "atomic" orbitals. The minimal basis set comprised atomic orbitals representing In^{1+} ($1s2s2p3s3p3d4s4p4d5s5p$) and N^{1-} ($1s2s2p$). We employed even-tempered Gaussian functions in the construction of the atomic orbitals. The s and p orbitals of In were described with 16 even-tempered Gaussian functions with the respective minimum and maximum exponents of 0.14 and 0.2300×10^6. The d orbitals for In entail 14 even-tempered Gaussian, the same as for the ones s and p at the exclusion of the two largest exponents. Similarly, the s and p orbitals of N were constructed using 13 even-tempered Gaussian exponents whose smallest and largest values were 0.124 215 and $0.136\,000\,5\times10^5$. The computations were generally completely self-consistent after 60 iterations. The convergence, for a given self-consistent calculation, was reached when the potential did not change by more than 10^{-5} from one iteration to the next. Upon reaching self-consistency, the error made in accounting for 72 electrons was 0.004 31.

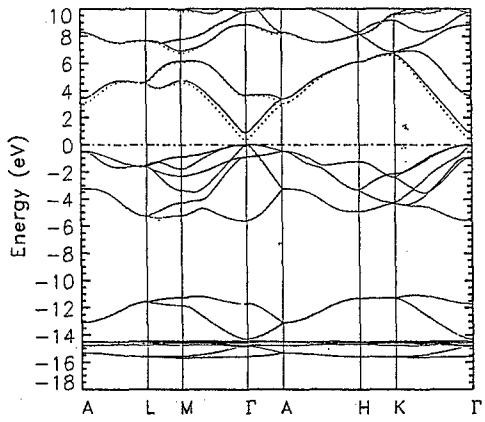

FIG. 1. LDA-BZW band structure of wurtzite indium nitride (InN). Lattice constants: a=3.544 Å, c=5.718 Å, and u=0.3790. The solid lines represent the band as obtained with the optimal basis set. The dotted lines show an example of bands resulting from calculations with basis sets larger than the optimal one. The Fermi level is set to zero. The occupied energies are the same in the two calculations.

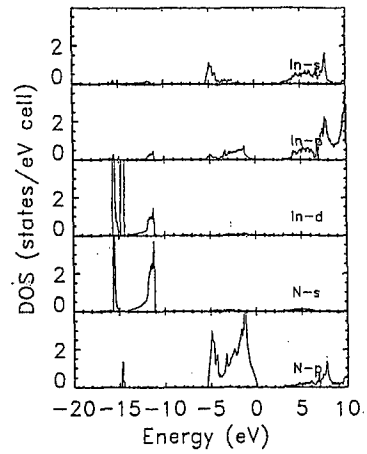

FIG. 3. Partial density of states (pDOS) for wurtzite InN as obtained from the bands (solid lines) shown in Fig. 1. The dominance of nitrogen p at the top of the valence band is obvious in this graph.

RESULTS

Our results for the energy bands, the total (DOS), and the partial densities of states (pDOS) are, respectively, shown in Figs. 1–3. The LDA-BZW bands are very similar to the ones obtained with GGA-BZW. The salient difference between these results and the findings of previous calculations resides in the description of the unoccupied bands. Indeed, these bands, as clearly explained above in relation to the Rayleigh theorem and the BZW method, do not suffer from the extra lowering ascribed to the basis set and variational effect elucidated by Bagayoko and co-workers.[34–38] It is important to note that the referenced lowering of some unoccupied bands is far from being rigid, i.e., it is highly dependent on the k point and is greatest for free-electronlike band (parabolic or not) and minimum for flat ones and at high symmetry points. Table I provides the energies at high symmetry points in the Brillouin zone. It is hoped that these data will lend themselves to further comparison of our results with experimental findings, including optical transition energies. The LDA-BZW calculated band gap of wurtzite indium nitride is 0.88 eV. The GGA-BZW gap is 0.81 eV. These values agree very well with the second and recent group of experiments described above.

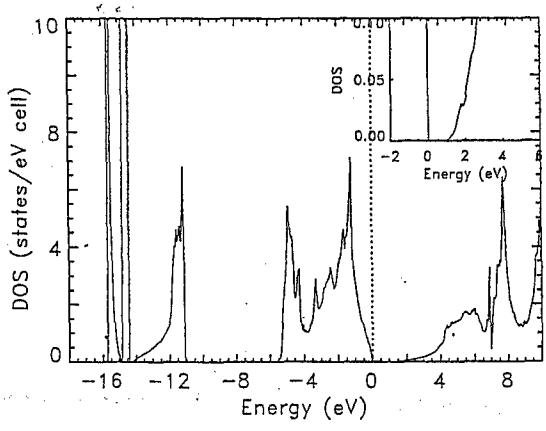

FIG. 2. Total density of states (DOS) for wurtzite indium nitride (InN) as obtained with the bands (solid lines) shown in Fig. 1. The inset supports our definition of a "practical band gap."

Bagayoko *et al.*[42] predicted the LDA band gaps of 0.65 and 0.74 eV for InN in the zinc-blende structure (c-InN), for the theoretical equilibrium (5.017 Å), and a low-temperature experimental (4.98 Å) lattice constants, respectively. These values are approximately 0.2 eV smaller than the above findings for wurtzite InN. Since the publication of these predictions,[42] we have come across the recent experimental findings[43] that somewhat agree with them, within the limitations associated with a high density of defects in the cubic layer, hexagonal inclusions up to 30% to the surface, and a very high carrier concentration above 10^{19} cm^{-3}. Indeed, Cimalla *et al.* reported,[43] within the preceding limitations, the results of optical investigations that indicated an absorption edge below 0.6 eV. The authors[43] recommended confirmation of this indication with a high-quality cubic InN.

Our group[34,35] introduced the concept of "practical band gap." Essentially, the practical band gap designates a range of values of the band gap, as per the inset of the total density-of-state (DOS) curve, such that an experimental measurement could produce results anywhere in that range, depending on the sensitivity of the apparatus and techniques, the fitting and interpretations of these results, and related uncertainties. Clearly, the inset in Fig. 2 shows that measurements, particularly optical absorptions, could lead to values of the band-gap ranging from the theoretical minimum of 0.88 to 2 eV. We certainly contend that the provided defects, impurities, and other factors (i.e., electron concentration) do not explain the relatively large band gap of w-InN as found by the first group of experiments, then the above concept of practical band gap does. Unlike the three-pronged approach of Wu *et al.*,[12–14] using highly sensitive techniques, optical absorption was generally the lone approach utilized in the early determinations of the band gap of w-InN. Even the 2004 results of Shubina *et al.*,[30] as mentioned earlier, are subject to this interpretation. Indeed, these authors identified a kink to denote the position of the band edge even though

TABLE I. Eigenvalues (eV), at some high symmetry points, for wurtzite indium nitride (w-InN) as obtained from LDA-BZW calculations for a=3.544 Å, c=5.718 Å, and u=0.3790. The Fermi energy of −0.222 12 eV is set to zero in the table.

A	L	M	H	K	Γ
−13.0972	−11.5668	−11.2329	−11.3021	−11.2827	−11.6988
−3.25532	−5.25538	−5.20231	−4.89999	−4.32501	−5.61294
−3.25532	−5.25538	−4.27059	−4.89999	−4.32501	−0.89662
−0.46069	−1.62671	−3.34893	−3.34349	−4.2695	−0.89662
−0.46069	−1.62671	−2.29475	−3.34349	−2.39761	−0.0049
−0.46069	−1.53365	−1.75651	−1.23894	−2.39761	0
−0.46069	−1.53365	−0.8656	−1.23894	−2.14019	0
3.366891	4.570732	4.748424	6.125875	6.740313	0.878663
3.367163	4.570732	6.175673	6.125875	6.740313	3.662409

the absorption, as per their Fig. 2(c) visibly commenced around 0.9 eV and reached a plateau at 2 eV, in accordance with our concept of practical band gap.

The LDA-BZW effective masses for the electron close to the bottom of the lowest conduction band at gamma show a slight anisotropy. The electron effective mass is around $0.088m_o$ in the plane perpendicular to k_z (from Γ to M and Γ to K) and $0.082m_o$, in the direction of k_z (from Γ to A), in the immediate vicinity of the gamma (Γ) point. The GGA-BZW calculations led to values of the electron effective mass very similar to the ones for LDA. Specifically, at the bottom of the lowest conduction band, they are 0.081, 0.077, and $0.082m_o$ from Γ to M, Γ to K, and Γ to A directions, respectively. These effective masses are also in agreement with experiment,[14] taking into account the quality and other features of the samples (i.e., temperature, pressure, electron concentrations). Wu *et al.*[14] obtained a value of 0.07 by using a band gap of 0.7 eV in their analysis. They also provided a plot of the electron effective mass as a function of electron concentration.

DISCUSSIONS

For a discussion of our results, we underscore the need for specificity relative to the lattice parameters, sample quality[30] and growth conditions,[11] temperature,[12] and electron concentration[11] when comparing results from different experimental investigations. In particular, the significant effect of electron concentration on the band gap[11,44–46] could explain the 0.75–0.8-eV band gap found by Wu *et al.*[12] whose samples had a relatively low electron concentration of 5×10^{18} cm^{-3}. Our calculated band gap of 0.88 eV agrees very well with the experimental result of 0.89 eV of Inishima *et al.*[11] for a sample with an electron concentration of 5×10^{19} cm^{-3}. As noted above in connection with the "practical band-gap," measurement techniques, the analysis of data, and related uncertainties are critical. Specifically, we reiterate that absorption techniques could lead to a value of the band gap of w-InN as large as 2 eV.

Some authors[22] evoked a p-d repulsion to explain the small (generally negative) band gap from previous LDA calculations. LDA is reported to overestimate this repulsion and to push upward the top of the valence band. Our results provide no indication of such a limitation of LDA. Rather, they clearly show that the extra lowering of the bottom of the conduction band, on account of the Rayleigh theorem, straightforwardly leads to the band-gap problem in LDA and other variational calculations that employ a basis set. This work partly responds to the calls by Ghani *et al.*[44] and by Vurgaftman and Meyer[45] for revisiting the issue of the band gap of w-InN following their extensive compilations of experimental and theoretical results on indium nitride. Ghani *et al.* discussed the formation of oxynitrides (InON), particularly in aged or annealed polycrystalline samples, as a possible source for the increase of the band gap to values around 2 eV. These polycrystalline films are reported to be susceptible to containing a high density of oxygen atoms at their grain boundaries.

CONCLUSION

In conclusion, we claim to have resolved the controversy surrounding the band gap of wurtzite InN. We did so within the local-density approximation (LDA) with the BZW method. Unlike many schemes purporting to correct limitations of local-density approximation and that come with other approximations whose effects are at best ill understood, the *ab initio* BZW method is rigorously anchored on a mathematical theorem. The above points explain the reason this communication is hoped to end the echoing of the incorrect chorus claiming that it is well known that local-density approximation woefully underestimates the band gap of semiconductors and insulators. In the above sense, and even though this communication is devoted to wurtzite InN, the method applies to other calculations that employ basis sets in a variational scheme of the Rayleigh–Ritz type, as is the case in many energy level (finite systems) or band calculations. An utterly important point associated with the above points stems from the fact that the proliferation of schemes aimed at "correcting" limitations of LDA has started to look like that of epicycles in the Ptolemaic model of the solar system. A seriously unfortunate consequence of this situation consists of diverting efforts from grasping the actual capabilities and limitations of LDA and those of schemes aimed at going beyond the local-density approximation or beyond density-functional theory altogether.

ACKNOWLEDGMENTS

This work was funded in part by the Department of the Navy, Office of Naval Research (ONR, Award Nos. N00014-98-1-0748 and N00014-05-1-0009), NASA (Award Nos. NCC 2-1344 and NAG 5-10253), the National Science Foundation (Award No. HRD 0000272), and by the Louisiana Board of Regents [Contract No. LEQSF(2002-03)-ENH-TR-57]. The authors are indebted to Dr. J. Wu for bringing the band-gap problem for *w*-InN to their attention. They also acknowledge the support and work of Dr. G. L. Zhao in the calculations of the atomic wave functions for In and N.

[1]J. W. Orton and C. T. Foxon, Rep. Prog. Phys. **65**, 1 (1998).
[2]O. Ambacher, J. Phys. D **31**, 2653 (1998).
[3]K. Osamura, S. Naka, and Y. Murakami, J. Appl. Phys. **46**, 3432 (1975).
[4]J. Hovel and J. J. Cuomo, Appl. Phys. Lett. **20**, 71 (1972).
[5]N. Puychevrier and M. Menoret, Thin Solid Films **36**, 141 (1976).
[6]V. A. Tygai, A. M. Evstigneev, A. N. Krasiko, A. F. Andreeva, and V. Ya. Malakhov, Sov. Phys. Semicond. **11**, 1257 (1977).
[7]T. L. Tansley and C. P. Foley, J. Appl. Phys. **59**, 3241 (1986).
[8]K. L. Westra, R. P. W. Lawson, and M. J. Brett, J. Vac. Sci. Technol. A **6**, 1730 (1988).
[9]Q. Guo and A. Yoshida, Jpn. J. Appl. Phys., Part 1 **33**, 2453 (1994).
[10]S. Yamagushi *et al.*, Appl. Phys. Lett. **76**, 876 (2000).
[11]T. Inishima, V. V. Mamutin, V. A. Vekshin, S. V. Ivanov, T. Sakon, M. Motokawa, and S. Ohoya, J. Cryst. Growth **227–228**, 481 (2002).
[12]J. Wu *et al.*, Appl. Phys. Lett. **80**, 3967 (2002); Also see V. Yu. Davydov *et al.*, Phys. Status Solidi B **229**, R1 (2002).
[13]J. Wu, W. Walukiewicz, K. M. Yu, J. W. Ager III, E. E. Haller, H. Lu, and W. J. Schaff, Appl. Phys. Lett. **80**, 4741 (2002).
[14]J. Wu, W. Walukiewicz, W. Shan, K. M. Yu, J. W. Ager III, E. E. Haller, H. Lu, and W. J. Schaff, Phys. Rev. B **66**, 201403 (2002).
[15]T. Matsuoka, H. Okamoto, M. Nakao, H. Harima, and E. Kurimoto, Appl. Phys. Lett. **81**, 1246 (2002).
[16]A. Kasic, M. Schubert, Y. Saito, Y. Nanishi, and G. Wagner, Phys. Rev. B **65**, 115206 (2002).
[17]B. Arnaudov *et al.*, Phys. Rev. B **69**, 115216 (2004).
[18]C. P. Foley and T. L. Tansley, Phys. Rev. B **33**, 1430 (1986).
[19]Y. C. Yeo, T. C. Chong, and M. F. Li, J. Appl. Phys. **83**, 1429 (1998).
[20]D. Fritsch, H. Schmidt, and M. Grundmann, Phys. Rev. B **67**, 235205 (2003). Please also see D. Fritsch, H. Schmidt, and M. Grundmann, *ibid.* **69**, 165204 (2004), where new empirical pseudopotentials produced band gaps of 0.790 and 0.824 eV for the anisotropically and isotropically screened potentials, respectively.
[21]M. van Schilfgaarde, A. Sher, and A. B. Chen, J. Cryst. Growth **178**, 8 (1997).
[22]F. Bechstedt and J. Furthmüller, J. Cryst. Growth **246**, 315 (2002).
[23]N. E. Christensen and I. Gorczyca, Phys. Rev. B **50**, 4397 (1994); Also see Z. Bridi, B. Bouhafs, and P. Ruterana, New J. Phys. **4**, 94.1 (2002), where the band gap is 0.17 eV.
[24]D. Vogel, P. Krüger, and J. Pollmann, Phys. Rev. B **55**, 12836 (1997).
[25]C. Stampfl and C. G. Van de Walle, Phys. Rev. B **59**, 5521 (1999).
[26]N. Farrer and L. Bellaiche, Phys. Rev. B **66**, 201203 (2002).
[27]S.-H. Wei, X. Nie, I. G. Batyrev, and S. B. Zhang, Phys. Rev. B **67**, 165209 (2003).
[28]M. H. Tsai, D. W. Jenkins, J. D. Dow, and R. V. Kasowski, Phys. Rev. B **38**, 1541 (1988).
[29]Y.-N. Xu and W. Y. Ching, Phys. Rev. B **48**, 4335 (1993).
[30]T. V. Shubina, S. V. Ivanov, V. N. Jmerik, D. D. Solnyshkov, V. A. Vekshin, and P. S. Kop'ev, Phys. Rev. Lett. **92**, 117407 (2004).
[31]D. M. Ceperley and B. J. Alder, Phys. Rev. Lett. **45**, 566 (1980).
[32]J. P. Perdew and A. Zunger, Phys. Rev. B **23**, 5048 (1981).
[33]J. P. Perdew and A. Zunger, Phys. Rev. B **23**, 5048 (1981); J. P. Perdew and W. Yue, *ibid.* **33**, 8800 (1986); J. P. Perdew, *ibid.* **33**, 8822 (1986).
[34]D. Bagayoko, G. L. Zhao, J. D. Fan, and J. T. Wang, J. Phys.: Condens. Matter **10**, 5645 (1998).
[35]G. L. Zhao, D. Bagayoko, and T. D. Williams, Phys. Rev. B **60**, 1563 (1999).
[36]D. Bagayoko, Int. J. Quantum Chem. **17**, 527 (1983).
[37]D. Bagayoko, G. L. Zhao, and S. Hasan, *in Contemporary Problems in Mathematical Physics*, edited by J. Govaerts, M. N. Hounkonnou, and A. Z. Msezane (World Scientific, London, 2002), pp. 222–232.
[38]G. L. Zhao, D. Bagayoko, and L. Wang, Phys. Rev. B **69**, 245416 (2004).
[39]P. J. Feibelman, J. A. Appelbaum, and D. R. Hamann, Phys. Rev. B **20**, 1433 (1979).
[40]B. N. Harmon, W. Weber, and D. R. Hamann, Phys. Rev. B **25**, 1109 (1982).
[41]G. L. Zhao, T. C. Leung, B. N. Harmon, M. Keil, M. Muller, and W. Weber, Phys. Rev. B **40**, 7999 (1989).
[42]D. Bagayoko, L. Franklin, and G. L. Zhao, J. Appl. Phys. **96**, 4297 (2004).
[43]C. Cimalla *et al.*, Superlattices Microstruct. **36**, 487 (2004).
[44]A. G. Bhuiyan, A. Hashimoto, and A. Yamamoto, J. Appl. Phys. **94**, 2779 (2003).
[45]I. Vurgaftman and J. R. Meyer, J. Appl. Phys. **94**, 3675 (2003).
[46]V. Y. Davidov *et al.*, Phys. Status Solidi B **230**, R4 (2002).

Manuscript submitted to Phys. Rev. B

Reexamination of the Ab-Initio Calculation of the Electronic Structure of ZnSe, Ge, and GaAs

G. L. Zhao*, L. Franklin and D. Bagayoko
Department of Physics, Southern University and A & M College
Baton Rouge, Louisiana 70813 USA

Abstract

In this work, we reexamined some of the mathematical and physical properties of the ab-initio LCAO calculations for the electronic structure of ZnSe, Ge, and GaAs. The utilization of non-strongly minimal systems in the self-consistent ab-initio calculations could lead to a non-uniformity in approaching the solution in the Ritz-process. We performed test computations for the electronic structure of hydrogen atom. We have proposed that an optimum basis set may be needed so that the calculated electron density is converged and the significant scattering of the Ritz-coefficients may be avoided. We have applied the new method to the calculations of the electronic structure of ZnSe, Ge, and GaAs. Our calculated results of the electronic properties agree well with experimental data.

1 Introduction

Ab-initio density functional calculation is a very powerful tool to study the physical properties of materials, including semiconductors, metals, surfaces, interfaces, and others.[1, 2, 3, 4, 5, 6, 7] However, previous density functional calculations in local density approximation (LDA) for semiconductors or insulators often underestimated the band-gaps by 30-50 %.[8, 9, 10, 11] Closely related to the band-gap problem, the calculated effective masses of electrons (n-type carriers) and the optical properties of semiconductors –from previous LDA computations– also disagree with experimental results. There have been some theoretical efforts intended to address these problems, including the calculations that utilize nonlocal, energy-dependent, non-Hermitian self-energy operators.[12, 13, 14, 15, 16, 17, 18] Others implemented the exact exchange potentials or included the effects of core states via the exchange diagram.[19, 20, 21] Aryasetiawan and Gunnarsson reviewed several computational methods, including the GW method, aimed at describing excited state properties.[17]. Johnson and Ashcroft recently utilized simplified applications of the GW method to make scissors-type corrections to the band gaps of semiconductors.[18]

In this work, we reexamine some of the mathematical properties of the self-consistent ab-initio density functional calculations that utilize the linear combination of atomic orbital (LCAO) formalism. We discuss the Ritz-process of the variational calculation that was implemented in the LCAO calculations and the related mathematical theorem. The identified mathematical properties of the Ritz-process, which is the foundation of the LCAO calculations, may be indispensable for understanding the band-gap and related problems for semiconductors. We performed test computations for the electronic structure of hydrogen atom. We will illustrate some of the mathematical and physical properties of the self-consistent ab-initio calculations of the Ritz-process by the results of the calculations on hydrogen atom, ZnSe, Ge, and GaAs.

In the next section, we summarize the computational method and the related mathematical properties. We present the calculated results in Section III, followed by a short conclusion in Section IV.

2 Method

2.1 The Kohn-Sham Equation and The Ritz Process in the LCAO Calculations

Our calculations of the electronic structure of materials are based on the density functional theory of Hohenberg-Kohn and Kohn-Sham.[1, 2] The Schrödinger-like equation, which is also known as the Kohn-Sham equation, of many electron system [1, 2, 3] is

$$\{-\frac{\hbar^2}{2m}\nabla^2 - \sum_{lm}\frac{e^2 Z_m}{\mid \vec{r}-\vec{\tau}_m-\vec{R}_l \mid} + e^2\int\frac{\rho(\vec{r}')}{\mid \vec{r}-\vec{r}' \mid}dv' + V_{xc}\}\Psi_{\vec{k}i} = E_{\vec{k}i}\Psi_{\vec{k}i} \quad (1)$$

where $E_{\vec{k}i}$ and $\Psi_{\vec{k}i}$ are the eigen-energy and eigen-function of the i-th electronic state at the $\vec{k}$-point in the Brillouin zone; $\vec{\tau}_m$ and Z_m are the position and nuclear charge of the m-th ion; $\vec{R}_l$ is a translational vector; V_{xc} is the exchange-correlation potential of the many-electron system. In this work, we employed a non-local density functional formalism of the exchange-correlation potentials in the generalized gradient approximation (GGA) that was developed by Perdew and Wang.[22] In fact, the Kohn-Sham equation is a non-linear differential equation, since the electron density $\rho(\vec{r})$ depends

on the wave functions $\Psi_{\vec{k}i}$ of the occupied electron states, i. e.,

$$\rho(\vec{r}) = \sum_{\vec{k}i} f_{\vec{k}i} \mid \Psi_{\vec{k}i} \mid^2 \tag{2}$$

where $f_{\vec{k}i}$ is the Fermi distribution function. The solution of the Kohn-Sham equation has to satisfy a condition that

$$\int \rho(\vec{r}) dv = N \tag{3}$$

where N is the total number of electrons in the system. In this work, we implemented the formalism of the linear combination of atomic orbitals method to solve the Kohn-Sham equation. The essentials of the mathematical properties of the calculations are those of the Ritz-process of the variational calculations. We will follow the notations in the discussion of the variational theory according to S. G. Mikhlin[23].

In the LCAO method,[24, 25, 26, 27, 28, 29, 30, 31, 32] we solve the Kohn-Sham equation self-consistly. We expand the eigenfunction $\Psi_{\vec{k}i}$ of the effective single electron state of the many-atom system as a linear combination of the atomic wave functions, which is a Ritz process as termed in the variational theory according to Mikhlin's notations.[23]

$$\Psi_{\vec{k}i}(\vec{r}) = \sum_{\alpha m} C_{\alpha m}(\vec{k}i) \phi_{\alpha m}(\vec{k}, \vec{r}) \tag{4}$$

where $C_{\alpha m}$ are the expansion coefficient or the Ritz-coefficients; $\phi_{\alpha m}(\vec{k}, \vec{r})$ are Bloch wave functions which are expressed in terms of atomic wave functions as

$$\phi_{\alpha m}(\vec{k}, \vec{r}) = \frac{1}{\sqrt{N}} \sum_{l} e^{i\vec{k}.\vec{R}_l} u_{\alpha m}(\vec{r} - \vec{\tau}_m - \vec{R}_l) \tag{5}$$

where $u_{\alpha m}$ is the atomic wave function of the α-th state of the m-th atom at the position $\vec{\tau}_m$ and is the coordinate element in the energy space (or Hilbert space). The solution for the Ritz-coefficients $C_{\alpha m}$ of the Kohn-Sham equation is the one that the total energy functional $E_{total}(\rho)$ reaches its minimum.

2.2 The Requirement of Strongly Minimal Systems in the Ritz Process

We shall study the countable system of the coordinate elements in the Hilbert space, where

$$\{u_n\} = u_1, u_2, u_3, ..., u_n, ... \tag{6}$$

The corresponding Gramm matrix of the first n-elements of $\{u_n\}$ is

$$R_n = \begin{pmatrix} (u_1,u_1) & (u_1,u_2) & ... & (u_1,u_n) \\ (u_2,u_1) & (u_2;u_2) & ... & (u_2,u_n) \\ ... & ... & ... & ... \\ (u_n,u_1) & (u_n,u_2) & ... & (u_n,u_n) \end{pmatrix} \tag{7}$$

where (u_i,u_j) can be an overlap matrix element in the LCAO formalism. The eigen-values of the Gramm matrix can be written in increasing order as

$$\lambda_1^n \leq \lambda_2^n \leq ... \leq \lambda_n^n \tag{8}$$

The system (Eq. (6)) is called strongly minimal in the energy space (Hilber space), if

$$inf\lambda_1^n = lim_{n\to\infty}\lambda_1^n > 0 \tag{9}$$

A relevant mathematical theorem for the Ritz-process in the variational calculation is the following: *In order for a Ritz-process to be stable, it is necessary and sufficient that its generating coordinate system* $\{u_i\}$ *be strongly minimal in the corresponding energy space.*[23]

In the LCAO calculations, the coordinate system, which is the basis set of the atomic orbitals, is not strongly minimal as required in the mathematical theorem. The problem is more obvious in some cases of the implementations of the basis sets such as 6-311G, 6-31G, or 5-31G. In those cases, some of the shell functions that describe the atomic states are not orthogonalized even on a single atomic site. In the solid state calculations, the smallest eigen-value of the overlap matrix could be negative in those calculations. As experienced by various researchers, the numerical instability problems could occur, which are usually referred as "linear dependency" problems.

In our implementations of the LCAO method, the atomic wave functions (or atomic orbitals) are obtained from ab-initio atomic computations. The atomic shell functions are orthogonal in the cases of free atoms or ions. However, the basis sets (or coordinate systems) of the atomic orbitals for the solid state calculations are neither orthogonal nor strongly minimal as that required by the above mentioned mathematical theorem. The problem is more intricate since we may notice the computational instabilities in the case that the problem becomes very severe, but we may not readily appreciate the beginning of the appearance of the computational instabilities. Particularly,

the onset of the computational instabilities in the LCAO method may not be marked by an occurrence of the negative eigen-value of the overlap matrix.

Mikhlin illustrated the problems of the utilization of non-strongly minimal systems in Ref. [23] by several examples. Generally, the non-strongly minimal systems will not reach a solution in the limit of $n \to \infty$ in the Ritz-process. For finite values of n, some of the non-strongly minimal systems may approximate the Ritz-coefficients with a tendency to stabilize non-uniformly for increasing n. Other non-strongly minimal systems may show that the Ritz-coefficients scatter significantly. The coefficients may change abruptly from one approximation to the next. One may not know the exact solution for the problem and has the difficulty of identifying an estimate for the error in the approximate solutions. There is so far no mathematical theorem that can identify exactly the properties of the instabilities in the utilization of non-strongly minimal systems in the Ritz-process. The relevant problems may include those such as the condition(s) that the instabilities may occur, the behavior of the instabilities, and the method(s) to identify them.

The problems became more complex in the applications of the numerical computations of the electronic structure of solid state materials, since most of the basis sets of various implementations of ab-initio density functional calculations are not strongly minimal. The true plane-wave basis set satisfies the condition to be strongly minimal. However, the requirement of the computational accuracy and the number of the true plane-waves in the solid state calculations are usually beyond the limitation of our computer resource at present. The orthogonalized plane waves, which are derived by the Schmitdt process to be orthogonal to the core wave functions, are not strongly minimal.

One may propose to orthogonalize the atomic orbitals for the solid state calculations. However, if the basis set is not strongly minimal, the orthogonalization of the basis set in solid state calculations may encounter the similar instability problem. The orthogonalization procedure of the basis set involves the computation of the inverse of the overlap matrix. If the smallest eigen-value of the overlap matrix approaches zero or negative, an instability problem may occur.

2.3 Consideration of Some Physical Properties

Although the true plane-wave basis set can be implemented in ab-initio density functional calculations of the electronic structure of solid state ma-

terials, the LCAO method is a much more efficient method in solving the Kohn-Sham equation of many-atom systems. The utilization of non-strongly minimal systems (or basis sets) such as those used in LCAO calculations could lead to either a divergent solution as $n \to \infty$, or could approach their solutions non-uniformly. The non-uniformity in approaching the solutions of the Ritz-process or the scattering of the Ritz-coefficients are particularly severe when the sizes of the basis sets become relatively large. This can be seen in the examples demonstrated by Mikhlin and were observed in previous ab-initio electronic structure calculations utilizing the LCAO method on various materials.[23, 30, 31]

In the cases that the ab-initio LCAO calculations or other similar ones are needed, we may utilize the considerations of some physical properties of the solid state materials in identifying approximate solutions without serious errors. One of the plausible hypotheses may be the following: If the exact solutions of the atomic wave functions for the atoms in the solid state are known, the required size n of the basis set is then determined by these atomic wave functions. There will be no need for any additional atomic orbitals (or atomic wave functions) in the corresponding energy space of the exact solution. However, we may not know the exact solutions of the atomic wave functions in the solid state in the practical calculations and may have to use an augmented basis set of atomic orbitals. We will address this problem in more detail in the next section when we present the calculation results. The difficulty may be lessened if a global self-consistent approach is implemented. We first calculate the atomic wave functions of free atoms in a neutral state. We use these atomic wave functions as the basis set to start the ab-initio calculation of the electronic structure of the solid. We then utilize the electronic structure of the solid state to estimate the charge transfer among the constituent atoms. The information is consequently utilized to identify the corresponding ionic state for a further refinement of the calculations. The global self-consistent procedure continues until the solutions converge.

3 Results

3.1 Test Calculations on Hydrogen Atom

In the calculations of the electronic structure of ZnSe, Ge, and GaAs, we implemented self-consistent ab-initio density functional computations that utilize the linear combination of atomic orbital formalism. To obtain the

atomic wave functions, we performed ab-initio atomic calculations that also utilized density functional formalism. The radial parts of the atomic wave functions were expanded in terms of a linear combination of Gaussian orbitals (LCGO).

The electronic energy levels and related wave functions of hydrogen atom are exactly known from the analytical solution of the Schrödinger wave equation. We can test the numerical performance of the variational computations of the Ritz-process on hydrogen atom. We utilized the same ab-initio atomic computation program and the LCGO formalism to calculate the electronic structure of hydrogen atom. The Schrödinger wave equation for the calculation of the electronic structure of hydrogen atom is a one-electron problem, instead of the many-body problems such as those for the studies of solid state materials. In the ab-initio computation of the hydrogen atom using the LCGO method, we did not include the density functional potentials in the Hamiltonian. The Schrödinger wave equation for hydrogen atom is then a linear differential equation, instead of the non-linear differential equation such as the density functional Kohn-Sham equation. We compared the results of the numerical computations of hydrogen atom with the exact solution. In the numerical computations, we utilized basis sets of even-tempered Gaussian exponentials with a minimum of 0.10×10^{-2} and a maximum of 0.15×10^{4} in atomic unit. We used various sizes of the basis sets of the Gaussian functions.

In Fig. 1, we present the calculated electronic energy levels of hydrogen atom versus the total numbers of the utilized Gaussian functions (Gaussian orbitals). The solid, dotted, and dash-dotted lines in Fig. 1 present the calculated energy levels of s-, p-, and d-states of hydrogen atom, respectively. As the numbers of the Gaussian functions in the basis sets increase from 5 to 15, the calculated energy levels approach their converged values. The calculated first three energy levels of hydrogen atom converged to -1.0, -0.250, and -0.111 Ry, when we utilized 15 – 60 Gaussian functions in the basis sets. These calculated energy levels of hydrogen atom agree very well with that of the exact solution for the principal quantum number $n = 1$, 2, and 3, respectively. The lowest energy level in Fig. 1 belongs to the 1s state of H atom. The second lowest level includes 2s and 2p states. The third one includes 3s, 3p, and 3d states.

When the numbers of the utilized Gaussian functions in the basis sets are larger than about 70, the calculated electron energy levels of the 3p and 3d states of hydrogen atom dropped to lower values than those of the exact solution. The features illustrate the instabilities of the variational calcu-

lations of the Ritz-process. Fig. 1 also shows that the numerical property of the instability in the computations of the 3d states of hydrogen atom is different from that of the 3p state. The calculated energy level of the 3d state of hydrogen atom dropped rapidly when the numbers of the utilized Gaussian functions in the basis sets are larger than about 70. The calculated energy level of the 3p state decreases much slowly, as compared with that of the 3d state in the same computations. The calculated energy level of 3s state remained the same as that of the exact solution in these test computations.

3.2 Electronic Properties of ZnSe

Zinc selenide (ZnSe) is a member of the II-VI family. Its crystal structure belongs to the space group of T_d^2. In these calculations, we used a lattice constant of $a = 5.65\mathring{A}$.[33, 34, 39] The formation of the Zn-Se bond has a partial ionic character in addition to its covalent bond. We first calculated the atomic wave functions of Zn^0 and Se^0. We utilized these atomic wave functions as the basis set to perform the ab-initio calculation of the electronic structure of ZnSe. The charge transfer in ZnSe was estimated from the calculated electronic wave functions. A Zn atom loses about 1.1 electrons to a Se atom. We then calculated the atomic wave functions of the ionic states of Zn^{1+} and Se^{1-}, utilizing self-consistent ab-initio atomic calculations. The radial parts of the atomic wave functions were expanded in terms of Gaussian functions. A set of even-tempered Gaussian exponentials was employed with a minimum of 0.15 and a maximum of 1.770×10^5. We used 18 Gaussian functions for the s and p states and 15 for the d states of Zn. We utilized 19 Gaussian functions for the s and p states and 17 for the d states of Se. In the self-consistent ab-initio calculations for the electronic structure of the solid state ZnSe, we included a mesh of 28 k-points, with proper weights in the irreducible Brillouin zone. We took the 1s, 2s, and 2p states of Zn and Se as the core states in the frozen core approximation, and allowed all other states to relax in the self-consistent ab-initio calculations. The computational error for the charge density was about 0.0023 for 44 electrons. The self-consistent potentials converged to a difference around 10^{-5} after about 60 iterations. The total number of iterations varies with the input potentials.

We performed five distinct calculations in order to determine the optimal basis set for the calculation of the electronic structure of ZnSe, utilizing the procedure as discussed in the above section and in the previous publications.[30, 31] Table 1 illustrates the atomic orbitals of the basis sets

of the five self-consistent calculations. We first carried out completely self-consistent calculations for ZnSe using a basis set that included Zn(1s2s3s4s 2p3p 3d) and Se(1s2s3s4s 2p3p4p 3d) orbitals. We then repeated the self-consistent calculation using the above basis set as augmented by the orbitals describing the next lowest-lying energy level of Zinc. Hence, Zn(4p) orbitals were added to basis set I. We then plotted the energy bands from these two distinct calculations, i.e., calculation I and II, and compared them numerically and graphically. Differences were obvious. We then performed calculation III and compared its results to those of calculation II. Up to five self-consistent calculations were performed and the results of each calculation were compared to those of the previous one as explained above.

In Fig. 2, we presnt the calculated electron energy bands of ZnSe from calculation III (solid lines) and calculation IV (dashed lines). Here $\Gamma = (0,0,0)$; $L = (1,1,1)\pi/a$; $X = (0,1,0)2\pi/a$; $K = (3/4,3/4,0)2\pi/a$.[35] The zero of the energy was set at the top of the valence bands. The calculated energies of the occupied valence bands and the unoccupied conduction bands converged to an average difference of several meV. The fourth calculation (the dashed line) of Fig. 2 gives sufficiently converged electron energy bands of ZnSe with respect to the size of the basis set. As we present in the following sections, the calculated electronic properties of ZnSe from calculation IV agree well with experimental data.

However, as we added more atomic orbitals in the calculations, the calculated electron energy bands of ZnSe drifted away from the converged results of calculation IV around the Γ-point. One may observe a computational behavior that is similar to that of the calculations for hydrogen atom. Fig. 3 shows the comparison of results from calculation IV (solid lines) and from calculation V (dashed lines). The calculated occupied energy levels converged with respect to the size of the basis set. However, some of the calculated unoccupied energy levels become lower than those of the calculation IV, as more atomic orbitals are added in the calculations. Different from the case of hydrogen atom, there was no an exact solution for the electronic structure of ZnSe as a reference. Various physical interpretations were devised to explain the numerical performance of the Ritz-process in the calculations. Some of them were believed to contribute in various aspects to the problem. In fact, the problem was previously claimed as the failure of density functional theory or the failure of local density functional calculations in many occasions. Part of the support for this claim was due to the fact that the calculated conduction band energies (or the band-gap energies) of semiconductors utilizing various computational methods often

were much lower than that of experimental results.

In spite of the fact that the mathematical properties of different computational methods are different, it can be proved that the basis sets used in those of the previous ab-initio calculations did not satisfy the requirement of the strongly minimal systems. Those include all-electron LAPW calculations, LMTO calculations, pseudopotentials orthogonalized plane wave methods, and ab-initio Gaussian orbitals or LCAO calculations. Briggs et al used multi-grid accelerations and a real-space grid as a basis in their calculations of the electronic structure of elongated diamond cell, an isolated C60 molecule, and a 32-atom cell of GaN.[36] As Briggs et al discussed in their article, the real-space grid implementation can also introduce a spurious dependence of the Kohn-Sham eigen-values, the total energy, and the ionic forces on the positions of the ions with respect to the real-space grid.

Nevertheless, the mathematical and physical properties of the ab-initio electronic structure calculations should be carefully examined. As we presented in the previous sections, the utilization of the non-strongly minimal systems of the basis sets also play a role for the problem. In principle, an exact solution cannot be reached as the size n of the basis set goes to infinity. The Ritz-coefficients may scatter significantly from one approximation to the next as n becomes large. However, the calculation of the occupied states has to satisfy the restriction of Eq. (3) which may restrict the scattering of the Ritz-coefficients of these states. The calculation of the unoccupied states do not have the restriction and the problem of the scattering of the Ritz-coefficients is particularly severe when the sizes of the basis sets become relatively large. We have proposed that an optimum basis set may be needed so that (a) the calculated electron density is converged, and (b) the significant scattering of the Ritz-coefficients is avoided. In the calculation of the electronic structure of ZnSe, we selected the basis set IV as the optimal one that lead to the converged electron density and related properties. The calculated electron energy bands are illustrated by the dashed line of Fig. 2 or by the solid lines of Fig. 3. One may observe that the calculated energy bands of the larger basis set (Calculation V in Fig. 3) are usually lower or unchanged as compared to those of the smaller basis set (Calculation IV in Fig. 3). This property can be understood from the Rayleigh theorem.[41, 42, 30, 31]

As shown in Fig. 2 and Fig. 3, ZnSe is a direct band gap semiconductor with the smallest gap energy of 2.6 eV at the center of the Brillouin zone (Γ). Our calculated band-gap energy is in good agreement with experimental measurements of about 2.8 eV.[34, 37, 38, 39] We present the total density

of states (DOS) of ZnSe in Fig. 4, as obtained from calculation IV. The total DOS curve in Fig. 4, particularly the inset, indicates that the small values of the density of states from 2.6 eV to 2.9 eV strongly suggest that measurements or related analysis that are not very sensitive may not detect the smallest energy gap.

Our calculated effective mass of n-type carriers, m_n^*, near the Γ-point is 0.15 m_0, where m_0 is the free-electron mass. This result is in good agreement with the experimental value of $0.16m_0$.[40, 39] The calculated effective mass of n-type carriers, away from the Γ-point, is between $0.15m_0$ and $0.17m_0$.

We also performed the self-consistent ab-initio calculations for the electronic structure of ZnSe, utilizing local density approximation for the exchange-correlation potential. We compared the electron energy bands from the LDA and GGA calculations. The average difference between the resulted bands of the two calculations is of the order of 1 mRy.

3.3 Electronic Structure of Ge

We performed the self-consistent ab-initio calculations for the electronic structure of crystalline Ge in the diamond structure. We used a zero temperature lattice constant of $a = 5.63\mathring{A}$ in these calculations.[39] We tested the convergency of the electronic structure calculation with respect to the size of the basis sets of atomic orbitals. We calculated the atomic wave function using a separate computer program that employed ab-initio density functional computations for atoms. We expanded the atomic wave functions as a linear combination of Gaussian orbitals (LCGO) in real space as discussed in the previous section.

In the calculation of the electronic structure of Ge, we employed non-local density functional potentials in the generalized gradient approximation that was developed by Perdew and Wang.[22] We first carried out completely self-consistent calculations for crystalline Ge using a basis set that included atomic orbitals of Ge(1s2s3s4s 2p3p4p 3d). We then repeated the self-consistent calculation using an augmented basis set that also included the orbital of Ge($4d^0$). In the self-consistent calculations of the electronic structure of solid Ge, we considered Ge(1s2s 2p) as the core states. All other states were treated as valence states and were allowed to relax in the self-consistent calculations. We then plotted the resulting energy bands from these two distinct self-consistent calculations. We observed that the occupied and unoccupied bands from the two calculations differ considerably.

The next step was to repeat our procedure for the third, fourth, and

fifth time. In these calculations, more atomic orbitals were added one at a time. The results of the fourth calculation (solid lines) and of the fifth calculation (dashed lines) are shown in Fig. 5, where the top of the valence bands is set as the zero of the energy. The fourth calculation included the atomic orbitals of Ge($1s^2 2s^3 3s^4 4s^2 5s^0$ $2p^6 3p^6 4p^6 5p^0$ $3d^{10} 4d^0$). The fifth calculation included an additional atomic orbital of Ge($5d^0$). The calculated electron energy bands from the fourth calculation do not have a noticeable difference from that of the fifth calculation for a large energy range from -13 eV to about 8 eV. The average difference between the occupied energy bands from the two calculations in Fig. 5 is of the order of several meV. The fourth calculation (the solid lines of Fig. 5) leads to sufficiently converged electron energy bands of crystalline Ge with respect to the size of the basis set.

We present the calculated energies (eV) of the electronic states of Ge at the selected high symmetry points in Table 2, along with some experimentally measured results. "Deg" in Table 2 refers to the degeneracy of the electronic states at that k-point. Our calculated results for the electronic energies agree very well with experimental values. The calculated, highest energy state of the valence bands is at the Γ-point. The lowest energy state of the conduction band is at the L-point. The calculated, indirect band gap is 0.62 eV, which agree well with experimental results of 0.66 - 0.74 eV.[39] In these calculations, we did not include the relativistic effects such as the spin-orbital interaction which will split the degenerate bands at the high symmetry points.

We listed the calculated effective masses of n-type carriers (electrons) in Table 3. Although the spin-orbital interaction only splits the electronic energy levels by a relatively small amount (of the order of about 20 meV), the curvature (dispersion) of the electron energy bands can change more noticeably. The calculated effective masses of p-type carriers (holes), without the consideration of the spin-orbital interaction in the calculations, can have a relatively large error and are not included in the Table 3. The lowest conduction band is not degenerate and the spin-orbital interaction may not affect substantially the effective masses of n-type carriers in this band. Our calculated effective masses of n-type carriers agree well with experimental results.[39]

We also compared the electron energy bands of Ge from the LDA and GGA calculations. The average difference between the energy bands, resulting from the two potentials, was approximately 1 mRy.

3.4 Electronic Structure of GaAs

We also applied the same calculation procedure as discussed in the previous sections to the study of the electronic structure of GaAs in the zinc blende structure. We used the experimental lattice constant of $a = 5.65\mathring{A}$ in the calculations.[43, 44] We calculated the atomic wave functions of Ga and As self-consistently. We evaluated the charge transfer in GaAs from the self-consistent ab-initio calculations of the electronic structure. Ga atoms in GaAs lose about 0.3 to 0.4 electrons per atom to As atoms. In the self-consistent ab-initio calculations, we employed non-local density functional potentials in the generalized gradient approximation. We used the 1s, 2s, and 2p states of Ga and As as the core states in the frozen core approximation, and allowed all other states to relax in the self-consistent ab-initio calculations. In Fig. 6, we present the calculated electron energy bands of GaAs along some high symmetry directions in the Brillouin zone. Here $\Gamma = (0,0,0)$; $L = (1,1,1)\pi/a$; $X = (0,1,0)2\pi/a$; $K = (3/4,3/4,0)2\pi/a$. The zero of the energy was set at the top of the valence bands. In Fig. 6, the solid lines represent the calculated results using the atomic orbitals of Ga(1s2s3s4s 2p3p4p 3d4d) and As(1s2s3s4s 2p3p4p 3d4d), where Ga(4d) and As(4d) are the unoccupied atomic orbitals. The dashed lines represent the calculated bands for the basis set that has an additional atomic orbital of As(5s). The calculated electron energy bands of the occupied states of GaAs from the two different calculations agree very well. The average difference of the energies of the occupied states from these two calculations is about several meV.

GaAs has a direct band-gap at the Γ-point as shown in Fig. 6. The lowest energy state of the conduction band is at the Γ-point. The lowest energy of the conduction band at the L-point is higher than that at the Γ-point by 0.2 eV. This result agrees well with the experimental value of 0.2 to 0.3 eV.[44] The theoretical band-gap energy of GaAs is 1.24 eV from this calculation. The reported experimental values of the band-gap energy of GaAs is 1.4 to 1.5 eV.[43, 44, 45] As we discussed in the previous sections, we present below the calculated electron density of states of GaAs in Fig. 7. There is a tail structure near the conduction band edge. The small values of the density of states from 1.24 eV to 1.7 eV strongly suggest that measurements or related analyses that are not very sensitive may not detect the smallest energy gap.

We also calculated the effective mass m^* of the electrons (n-type carriers) in the lowest conduction band near the Γ-point. The effective mass m^* is calculated from the curvature of the band dispersions. The calculated

effective mass of the electrons do not show much difference in the three directions that include $L \rightarrow \Gamma$, $X \rightarrow \Gamma$, and $K \rightarrow \Gamma$. They are 0.067, 0.068, and 0.068 m_0, respectively. The average value of the effective mass of the electrons is $m^* = 0.068 m_0$, where m_0 is the free electron mass. The experimental value of the effective mass m^* of the electrons is about 0.065 to 0.069 m_0.[44] Our calculated results agree well with the experimental data.

We compared the electron energy bands of GaAs from the LDA and GGA calculations. The average difference between the energy bands of the LDA and GGA calculations is of the order of 1 mRy.

4 Conclusion

In this article, we reexamined some of the mathematical and physical properties of the ab-initio density functional calculations for the electronic structure of ZnSe, Ge, and GaAs. We also performed test computations for the electronic structure of hydrogen atom. The utilizations of non-strongly minimal systems in the self-consistent ab-initio LCAO (or LCGO) calculations could lead to the non-uniformity in approaching the solutions in the Ritz-process. We are not aware a previous research article that fully addressed these problems. We have utilized a global self-consistent approach to determine the optimal basis sets for the calculation of the electronic structure of ZnSe, Ge, and GaAs. Our calculated results of the electronic properties agree well with experimental data.

Acknowledgment: This work was funded in part by the National Aeronautics and Space Administration (NASA, Award No. NCC 2-1344), the Department of the Navy, Office of Naval Research (ONR) [Grant No: N00014-05-1-0009], and the National Science Foundation and the Louisiana Board of Regents (NSF Award Nos. HRD-0000272 and LEQSF(2002-2003)-ENH-TR-57), partly through the Louis Stokes Louisiana Alliance for Minority Participation. The authors are grateful to Dr. S. Hasan for his excellent service of the computer facilities that were needed for this work.

* (E-mail) zhao@grant.phys.subr.edu

References

[1] P. Hohenberg and W. Kohn, Phys. Rev. **136**, B864 (1964).

[2] W. Kohn and L. J. Sham, Phys. Rev. **140**, A1133 (1965).

[3] J. Callaway and N. H. March, *Solid State Physics*, **38**, edited by H. Ehrenreich, D. Turnbull, and F. Seitz, (Academic Press, New York, 1984), p135, and references therein.

[4] M. L. Cohen, Science, **261**, 307 (1993).

[5] W. Y. Ching, J. Amer. Ceramic Soc. **73**, 3135 (1990).

[6] *Theory of the Inhomogeneous Electron Gas* 1983, edited by S. Lundqvist and N. H. March (Plenum, New York), and references therein.

[7] *Electronic Structure, Dynamics, and Quantum Structural Properties of Condensed Matter* 1985, edited by J. T. Devreese and P. van Camp, vol. 121 of NATO Advanced Study Institute. Series B: Physics (Plenum, New York), and references therein.

[8] G. B. Bachelet and N. E. Christensen, Phys. Rev. B **31**, 879 (1985).

[9] M. Rohlfing, P. Krüger and J. Pollmann, Phys. Rev. B **48**, 17791 (1993).

[10] L. J. Sham and M. Schlüter, Phys. Rev. Lett. **51**, 1418 (1985); Phys. Rev. B **32**, 3883 (1985).

[11] J. P. Perdew and M. Levy, Phys. Rev. Lett. **51**, 1884 (1985).

[12] M. S. Hybertsen and S. G. Louie, Phys. Rev. Lett. **55**, 1418 (1985); Phys. Rev. B **34**, 5390 (1986).

[13] X. Zhu and S. G. Louie, Phys. Rev. Lett. **56**, 2415 (1986).

[14] M. Rohlfing, P. Krüger and J. Pollmann, Phys. Rev. B **48**, 17791 (1993).

[15] O. Zakharov, A. Rubio, X. Blase, M. L. Cohen, and S. G. Louie, Phys. Rev. B **50**, 10780 (1993).

[16] M. Oshikiri and F. Aryasetiawan, Phys. Rev. B **60**, 10754 (1999).

[17] F. Aryasetiawan and O. Gunnarsson, Rep. Prog. Phys. **61**, 237 (1998).

[18] K. A. Johnson and N. W.Ashcroft, Phys. Rev. B **58**, 15548 (1998).

[19] M. Städele, M. Moukara, J. A. Majewski, P. Vogl, and A. Görling, Phys. Rev. B **59**, 10031 (1999).

[20] A. Fleszar, Phys. Rev. B **64**, 245204 (2001).

[21] W. Wu and A. G. Eguiluz, Phys. Rev. Lett. **89**, 126401 (2002).

[22] J. P. Perdew and Wang Yue, Phys. Rev. B 33, 8800 (1986); J. P. Perdew, Phys. Rev. B 33, 8822 (1986); J. P. Perdew and A. Zunger, Phys. Rev. B 23, 5048 (1981).

[23] S. G. Mikhlin, "The Numerical Performance of Variational Methods", (Wolters-Noordhoff Publishing, Groningen, Netherlands, 1971).

[24] P. J. Feibelman, J. A. Appelbaum and D. R. Hamann, Phys. Rev. B **20**, 1433 (1979).

[25] B. N. Harmon, W. Weber and D. R. Hamann, Phys. Rev. B **25**, 1109 (1982).

[26] W. Y. Ching, Y. Xu, G. L. Zhao, K. W. Wong and F. Zandiehnadem, Phys. Rev. Lett. **59**, 1333 (1987).

[27] G. L. Zhao, T. C. Leung, B. N. Harmon, M. Keil, M. Muller, and W. Weber, Phys. Rev. B. **40**, 7999 (1989).

[28] G. L. Zhao and B. N. Harmon, Phys. Rev. B **45**, 2818 (1992).

[29] G. L. Zhao and M. E. Bachlechner, Phys. Rev. B, **58**, 1887 (1998).

[30] D. Bagayoko, G. L. Zhao, J. D. Fan, and J. T. Wang, Journal of Physics: Condensed Matter, **10**, 5645 (1998).

[31] G. L. Zhao, D. Bagayoko, and T. D. Williams, Physical Review B **60**, 1563 (1999).

[32] N. E. Brener, J. M. Tyler, J. Callaway, D. Bagayoko, and G. L. Zhao, Physical Review B **61**, 16582 (2000).

[33] C. Kittel, Introduction to Solid State Physics, 7-th Ed, (John Wiley & Sons, New York, 1996), Ch. 1.

[34] See, for example, the review article by H. Morkoc, S. Strite, G. B. Gao, M. E. Lin, B. Sverdlov and M. Burns, J. Appl. Phys. **76**, 1363 (1994).

[35] J. Callaway, Quantum Theory of the Solid State, (Academic Press, New York, 1976).

[36] E. L. Briggs, D. J. Sullivan, and J. Bernholc Phys. Rev. B **52**, R5471 (1995).

[37] T. L. Chu, S. S. Chu, G. Chen, J. Britt, C. Ferekides, and C. Q. Wu, J. Appl. Phys. **71**, 3865 (1992).

[38] J. Z. Zheng and J. W. Allen, Phys. Rev.B. **49**, 7770 (1994).

[39] Landolt-Börnstein New Series III, vol. 22a, *Zahlenwerte und Funktionen aus Naturwissenschaften und Technik*, edited by O. Madelung, (Springer, New York, 1987).

[40] P. J. DEAN, D. C. HERBERT, A. M. LAKEE, Proc. 15th Int. Conf. Physics of Semiconductors , Kyoto, J. Phys. Soc. Jpn. **49**, Suppl. A, 185 (1980).

[41] S. H. Gould, *"Variational Methods for Eigenvalue Problems"*, (University of Toronto Press, 1957), ch. 2.

[42] D. Bagayoko, Inter. J. of Quantum Chemistry **17**, 527 (1983).

[43] S. Adachi, J. Appl. Phys. **58**, R1-R29 (1985).

[44] Landolt-Börnstein New Series III, vol. 17a, *Zahlenwerte und Funktionen aus Naturwissenschaften und Technik*, edited by K. H. Hellwege and O. Madelung, (Springer, Berlin, 1982).

[45] A. R. Goni, A. Cantarero, K. Syassen, and M. Cardona, Phys. Rev. B **41**, 10111 (1990).

Table 1: The atomic orbitals in the basis sets of the five distinct calculations for the electronic structure of ZnSe.

Basis	Zn core	Se core	Zn valence	Se valence
I	1s2s 2p	1s2s 2p	3s4s 3p 3d	3s4s 3p4p 3d
II	1s2s 2p	1s2s 2p	3s4s 3p4p 3d	3s4s 3p4p 3d
III	1s2s 2p	1s2s 2p	3s4s 3p4p 3d	3s4s 3p4p 3d4d
IV	1s2s 2p	1s2s 2p	3s4s 3p4p 3d4d	3s4s 3p4p 3d4d
V	1s2s 2p	1s2s 2p	3s4s 3p4p 3d4d	3s4s5s 3p4p 3d4d

Table 2: Calculated electronic energies (eV) of Ge at the selected high symmetry points. The experimental data are from Reference [39, 44].

Ge	Calculation	Deg	Measurements
Γ_{1v}	-12.59	1	-12.6, -12.9±0.2
Γ'_{25v}	0.0	3	0.0
Γ'_{2c}	0.83	1	0.89
Γ_{15c}	2.81	3	3.01
L'_{2v}	-10.41	1	-10.6±0.5
L_{1v}	-7.44	1	-7.7±0.2
L'_{3v}	-1.39	2	-1.4±0.3
L_{1c}	0.62	1	0.74
L_{3c}	4.02	2	4.3±0.2, 4.2±0.1
L'_{2c}	8.29	1	7.8±0.6, 7.9±0.1
X_{1v}	-8.64	2	-9.3±0.2
X_{4v}	-3.00	2	-3.15±0.2, -3.5±0.2
X_{1c}	1.04	2	1.3±0.2
X_{3c}	9.98	2	
E_g	0.62		0.66, 0.74

Table 3: The effective masses (in m_0) of the n-type carriers at the lowest conduction band of Ge in the diamond structure.

	calculation	measurements
$m_{n\perp}(L_{1c})$	0.086	0.0807[39]
$m_{n\|\|}(L_{1c})$	1.43	1.57[39]
$m_{n\Gamma}$	0.043	0.038[39]

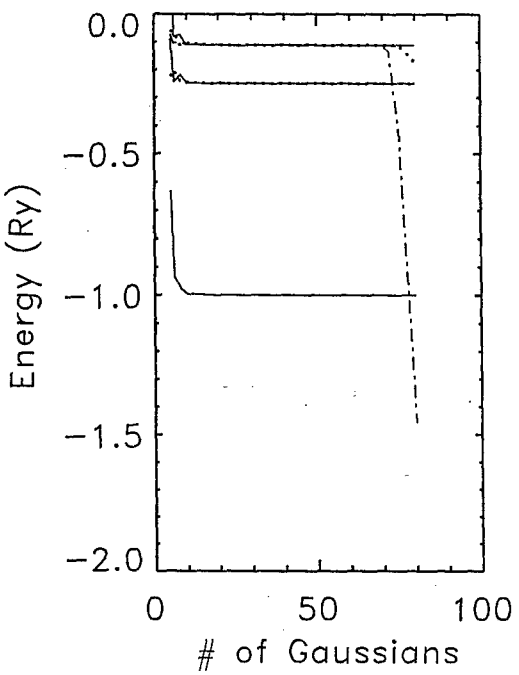

Figure 1: The calculated electronic energy levels of hydrogen atom versus the total numbers of the utilized Gaussian functions. The solid, dotted, and dash-dotted lines present the calculated energy levels of s-, p-, and d-states of hydrogen atom, respectively.

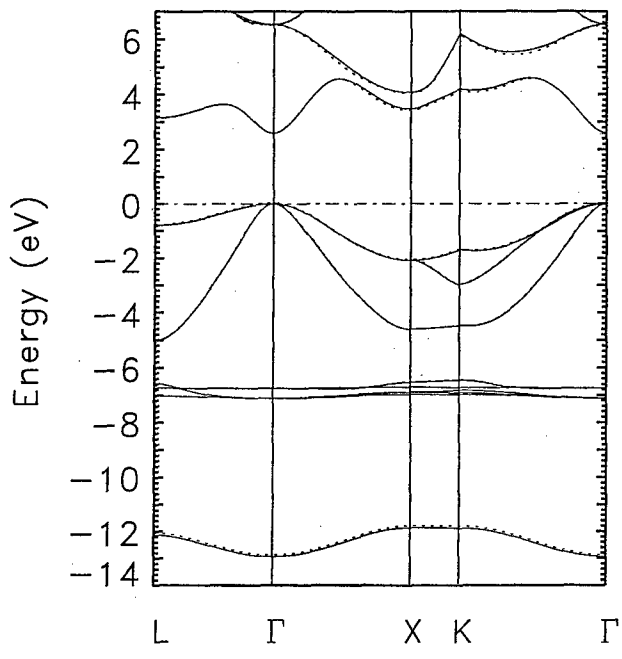

Figure 2: The calculated electronic energy bands of ZnSe along the high symmetry directions. The solid and dashed lines represent the results of calculations III and IV, respectively.

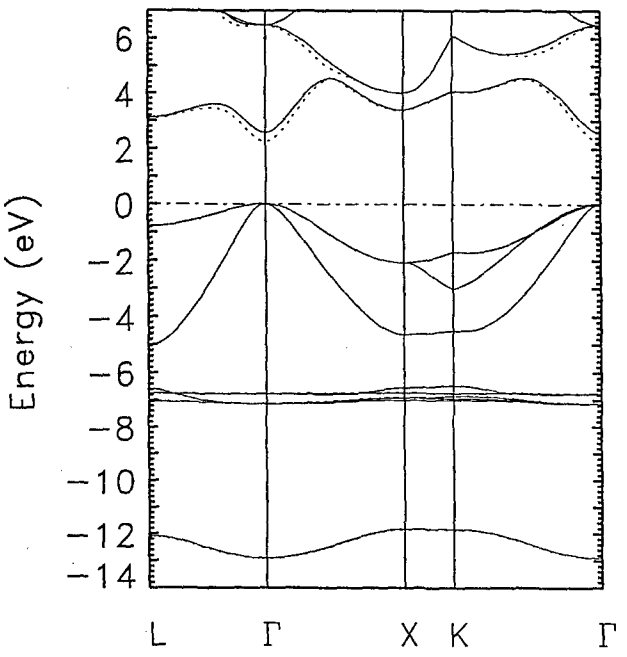

Figure 3: The calculated electronic energy bands of ZnSe from Calculation IV (solid lines) and Calculation V (dashed lines).

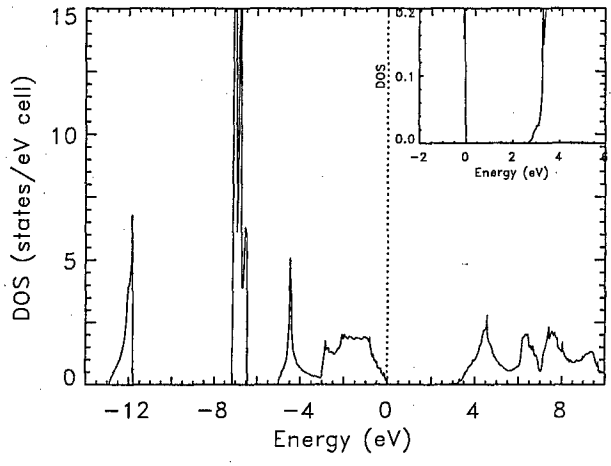

Figure 4: The calculated density of states of ZnSe. The inset shows the tail structure of the density of states of ZnSe near the bottom of the conduction bands.

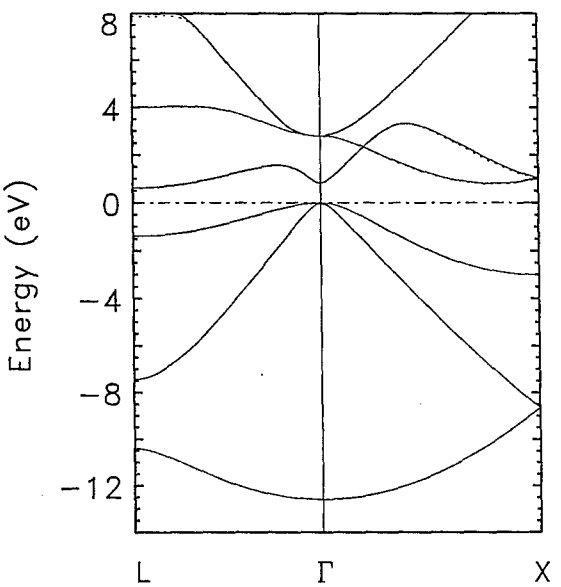

Figure 5: The calculated electronic energy bands of Ge along the high symmetry directions. The solid and dashed lines represent the results of the fourth and fifth calculations, respectively.

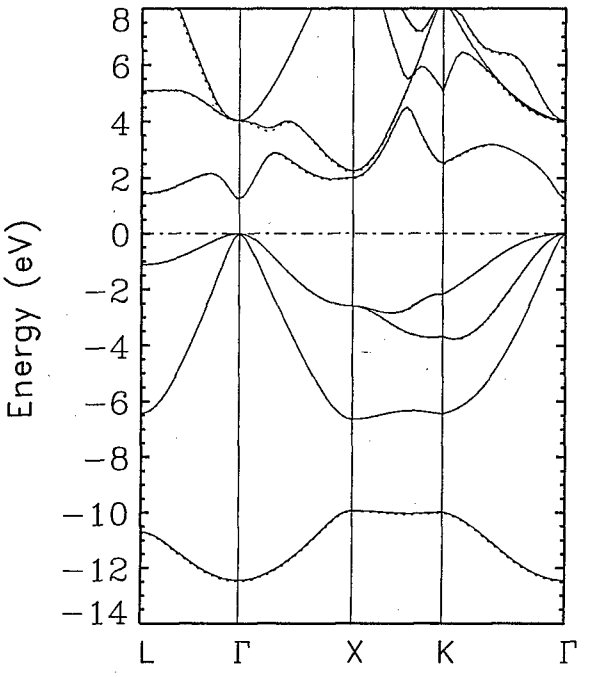

Figure 6: The calculated electron energy bands of GaAs.

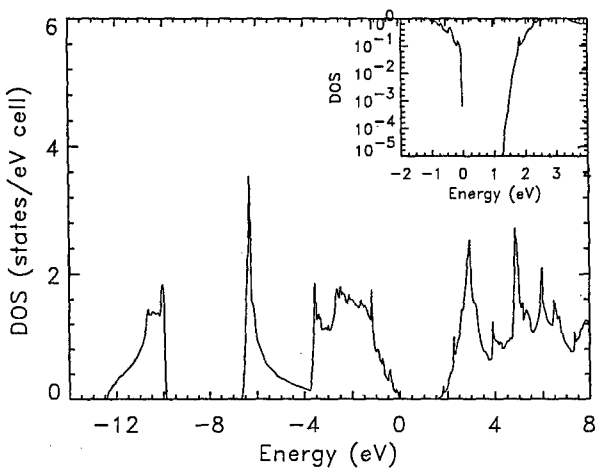

Figure 7: The calculated density of states of GaAs. The inset shows the tail structure of the density of states of GaAs near the bottom of the conduction bands.